

UC Irvine

UC Irvine Electronic Theses and Dissertations

Title

Space Radiation Effects: Comparison of Ovarian Toxicity of Low dose Gamma Radiation vs High LET Charged Particle Radiation

Permalink

<https://escholarship.org/uc/item/0d41q7tk>

Author

Awodele, Oluseyi A.

Publication Date

2021

Peer reviewed|Thesis/dissertation

UNIVERSITY OF CALIFORNIA,
IRVINE

Space Radiation Effects: Comparison of Ovarian Toxicity of Low Dose Gamma Radiation vs
High LET Charged Particle Radiation

THESIS

submitted in partial satisfaction of the requirements for
the degree of

MASTER OF SCIENCE

In Environmental Health Sciences

By

Oluseyi Awodele

Thesis Committee:
Professor Ulrike Luderer, Chair
Professor Charles Limoli
Professor Masashi Kitazawa

DEDICATION

To

Elizabeth Awodele, the Awodele family, the O'keefe family and friends
especially Dr. Dionicio Siegel for their unwavering support and commitment.

TABLE OF CONTENTS

	Page
LIST OF ABBREVIATIONS	v
LIST OF FIGURES	vii
LIST OF TABLES	viii
ACKNOWLEDGEMENTS	ix
ABSTRACT OF THE THESIS	x
CHAPTER 1: INTRODUCTION AND PURPOSE	1
CHAPTER 2: LITERATURE REVIEW	8
CHAPTER 3: METHODOLOGY	28
CHAPTER 4: RESULTS	32
CHAPTER 5: DISCUSSION	48
CHAPTER 6: CONCLUSION	56
REFERENCES	57

	LIST OF ABBREVIATIONS
AAALACI	American Association for the Accreditation of Laboratory Animal Care Facilities International
ACTH	Adenocorticotrophic Hormone
ANOVA	Analysis Of Variance
ATM	Ataxia Telangiectasia-Mutated
BRCA 1	Breast Cancer Susceptibility Gene 1.
cGy	Centi Gray
COX	Cyclooxygenase
DNA	Deoxyribonucleic Acid
DSBs	Double Strand Breaks
EPA	Environmental Protection Agency
FSH	Follicle-Stimulating Hormone
GCR	Galactic Cosmic Radiation
GnRH	Gonadotropin-Releasing Hormone
HR	Homologous Recombination
HZE	High Charge and Energy Particles
iNOS	Inducible Nitric Oxide Synthase
IR	Ionizing Radiation
JNK	C-Jun N-Terminal Kinase
keV	Kilo Electron Volts
LET	Linear Energy Transfer
LH	Luteinizing Hormone

NASA	National Aeronautics and Space Administration
NCRP	National Council on Radiation Protection
NF- κ B	Nuclear Factor Kappa B
NHEJ	Non-Homologous End Joining
PUMA	P53 Upregulated Modulator of Apoptosis
RNA	Ribonucleic Acid
SSBs	Single Strand Breaks
TGF	Transforming Growth Factor
TNF- α	Tissue Necrosis Factor Alpha
TSH	Thyroid Stimulating Hormone

LIST OF FIGURES

			Page
Figure 1a	Comparison of charged particle tracks in nuclear emulsions.		10
Figure 1b	Comparison of particle tracks in human cell nucleus immunostained for detection of γ -H2AX.		10
Figure 2	Image of Cell Cycle with checkpoints		14
Figure 3	Stages of Folliculogenesis		19
Figure 4	Schematic of Experimental design		29
Figure 5	Effects of gamma irradiation on whole body weight		33
Figure 6	Effects of gamma irradiation on measured weight of paired ovary+oviduct		34
Figure 7	Effects of gamma irradiation on measured wet uterus weight		35
Figure 8	Pictographic illustration of ovary rearrangements after discovery of error.		37
Figure 9	Histological hematoxylin and eosin staining of primordial, primary and secondary follicles.		38
Figure 10	Primordial follicles count (version 1 data result).		40
Figure 11	Primary follicles count (version 1 data result).		41
Figure 12	Secondary follicles count (version 1 data result).		42
Figure 13	Primordial follicles count (version 2 data result).		45
Figure 14	Primary follicles count (version 2 data result).		46
Figure 15	Secondary follicles count (version 2 data result).		47

	LIST OF TABLES	
		Page
Table 1	Career Exposure Limits for NASA Astronauts by Age and Gender	15
Table 2	Comparison of various space mission, their duration and observed radiation dose.	15
Table 3	Theoretical Career Effective Dose Limits for 1-year missions based on 3% REID (Average Life-loss for an Exposure-induced Death) for Radiation Carcinogenesis (1 mSv = 0.1 rem)	16
Table 4	Summary statistics, Gamma ray dose vs. measured variables (total body weight, wet uterus and paired ovary + oviduct)	32
Table 5	Summary data of follicle count per gamma dose exposure.	39
Table 6	Summary data of follicle count per gamma dose exposure (Rearranged slides).	44

ACKNOWLEDGEMENTS

I would like to thank my thesis committee chair, Professor Ulrike Luderer, and the members of my committee, Professor Charles Limoli and Associate Professor Masashi Kitazawa, for their guidance in this research project and for their mentorship throughout the Environmental Health Sciences graduate program and the Occupational and Environmental Medicine residency program at UC Irvine. I would also like to thank Dr. Alya Khan, the residency program director, for her ongoing mentorship and support.

ABSTRACT OF THE THESIS

Space Radiation Effects: Comparison of Ovarian Toxicity of Low Dose Gamma Radiation vs
High LET Charged Particle Radiation

By

Oluseyi Awodele

Master of Science in Environmental Health Sciences

University of California, Irvine 2020

Professor Ulrike Luderer, Chair

The biological effects of ionizing radiation on female reproduction have relatively been understudied. Currently about 30 percent of astronauts are women, and 46% of the 2017 NASA astronaut class are women. Astronauts are exposed to galactic cosmic rays (GCR) during travel in deep space. Galactic cosmic radiation is the dominant source of radiation that originates outside the earth's solar system. And must be dealt with aboard current spacecraft and future space missions within our solar system. It permeates interplanetary space and can pass practically unimpeded through a spacecraft or the skin of an astronaut. GCR consist of protons,

alpha particles, high-energy and highly charged ions called HZE particles and electrons. When GCR interacts with the gases within interstellar space, gamma radiation is also emitted. In assessing the reproductive toxicity risks to female astronauts, the premise that HZE particles have greater relative biological effectiveness than gamma radiation for ovarian toxicity has not been directly tested.

Recently published studies investigated the effects of high LET ^{56}Fe and ^{16}O particles in mice of the same strain and age (Mishra et al., 2016 and 2017). Both studies demonstrated profound sensitivity of the ovary to high-LET charged ion irradiation, with more than half of the irreplaceable ovarian follicle reserve destroyed 1 week after low dose irradiation. Comparison of prior studies suggest that high LET radiation may be a more potent inducer of ovarian follicle depletion than photon radiation, but existing published data sets did not utilize low enough doses of photon radiation to model the dose-response for these endpoints. In the current study, we present a comparison study investigating gamma radiation-induced dose dependent follicular destruction and relative biological effectiveness using same mice strain and age. 3-month-old female C57BL/6J mice were gamma-irradiated (0, 5, 15, and 50 cGy) using a ^{137}Cs source and euthanized 1 week after irradiation. Ovaries were collected and fixed in Bouin's fixative at necropsy and were embedded in paraffin. Ovaries were then serially and completely sectioned at 5 μm thickness. Sections were stained with hematoxylin and eosin. Ovarian follicles were counted using light microscopy, blinded to the treatment group. We hypothesized that 1) gamma radiation will cause dose dependent ovotoxicity and morphological reduction in ovarian size and 2) ovarian follicle destruction from gamma radiation will be less potent than high charged high LET particle radiation. Result: ^{137}Cs gamma radiation induced statistically significant reduction in measured total body in irradiated mice. Preliminary histomorphometric counts of 15 out of 32

ovaries shows 50cGy resulted in a dramatic total destruction of primordial and primary ovarian follicles after 1 week of irradiation, while follicle counts after 5 and 15 cGy did not differ from unirradiated controls.

CHAPTER 1: INTRODUCTION AND PURPOSE

The biologic effects of ionizing radiation (IR) on female reproduction have been relatively understudied. This data gap has become increasingly important as increasing numbers of women have joined the labor workforce, the use of IR-generating diagnostic medical devices, medical interventional procedures and anticancer treatments, advancements in air and space transportation, and increasing interest in nuclear power generation.

For the general public, the natural environment is still the highest source of ionizing radiation compared to other sources such as medicine, occupational and consumer products (NCRP 2009). Natural background ionizing radiation sources are products of radioactive decay of uranium, thorium, and potassium (Shahbazi-Gahrouei et al., 2013). Environmental Protection Agency (EPA) reports that the average annual radiation dose per each American is 6.2 millisieverts or 620 millirem of which 48% comes from medical procedure exposures. Occupational exposure accounts for <0.1 %. However certain occupations are exposed to higher-than-average levels of ionizing radiation (UNSCEAR 2000). For example, astronauts are exposed to significantly more radiation. Crews aboard the International Space Station (ISS) received an average of between 80 to 160 mSv for a six-month rotation depending on the solar environment (solar minimum vs solar maximum) (Rask et al., 2008). Solar minimum is the period with the minimum number of sunspots and a minimum solar magnetic field while solar maximum is the period of time with the maximum amount of sunspots and maximum solar magnetic field (Rask et al., 2008). National Aeronautics and Space Administration (NASA) estimates a total radiation dose of 1200 mSv for the planned 3-year Mars mission. (Dietze et al. 2013).

The first woman who traveled to space was Russian Cosmonaut Valentina Tereshkova in 1963. (Gibson 2014). Sally Ride became the first American woman astronaut in 1983. The percentage of female astronauts has steadily increased since 1978, when NASA graduated the first female astronauts. The number of women admitted to the NASA training program continues to grow (Jennings et al., 2000). In 2012, a total of 55 women had already been to space. 43 of them were Americans. (Gibson 2014). As of March 2020, the number has increased to 65 women (NASA website 2020). The ratio of female to male astronauts in NASA 2013 and 2017 graduating class were 50:50 and 45:55 respectively, which was a significant change compared to 33% female in 2009. During deep space missions, astronauts are exposed to high energy galactic cosmic radiation, which contains protons, neutrons, helium ions and ions heavier than helium (Rask et al., 2008).

OVERVIEW OF IONIZING RADIATION

The difference between ionizing versus nonionizing radiation is that IR has the ability to eject an electron from an atom's orbit, creating an ion or charged atoms in the process. Sources of IR include either natural radioactive decay or man-made. The five major environmental sources of IR include natural radioactive decay; medical; consumer products, residual fallout from nuclear weapon testing; and nuclear power energy (Eisenbud 1984). IR is divided into charged particle radiation (alpha, beta), uncharged particle (neutrons) or electromagnetic radiation (gamma and x-ray). These types of IR are further subdivided by their direct vs indirect ionization effects and ionizing density (Keith et al., 1999). In direct ionizing radiation, the radiation causes significant direct ionization (i.e., linear energy transfer). Examples are alpha and beta particle radiations. Indirect ionizing radiation is

electrically neutral and produces small primary ionization; however, it is the liberated electrons that produce damaging secondary ionization (Keith et al., 1999). Examples: neutron, gamma, or x-ray radiation. Linear energy transfer (LET) is defined as the rate of energy (E) deposition on an absorbing medium per unit distance (l) travelled by the radiation. i.e. $L = dE/dl$ and represented as $L = \text{keV}/\mu\text{m}$. (keV: kilo electron volts; μm : micrometers). The extent of biological damage is determined by the LET (Ray 2017).

Alpha radiation: is released during alpha radionuclide decay in which an alpha particle is released. Alpha particle is composed of two protons and two neutrons (i.e., helium) and is positively charged. Alpha particles are heavier (7200 times the size of an electron), highly charged, slow moving with high LET. They cause localized direct damage to a cell but due to their size have the lowest penetrating power compared to other types of radiation. They do not penetrate past the stratum corneum of the skin and pose no significant external exposure hazard (Keith et al., 1999).

Beta radiation: Beta particles are released during beta decay, in which an unstable atomic nucleus releases an electron (negatively charged) or positron (positively charged) from its nucleus. Beta particles have high velocity, are classified as low LET and have slightly higher penetrating power than alpha particles. (Keith et al., 1999).

HZE particles : Galactic cosmic radiation (GCR) is the dominant source of radiation that originates outside the earth's solar system. GCR contains nuclei of atoms without their surrounding orbital electrons and traveling at the speed of light. When GCR interacts with the gas within the interstellar space, it emits gamma radiation (Rask J. et al., 2008). GCR consists of 98% baryons and 2 % electrons. These baryons are composed of 85% protons (hydrogen nuclei), 14% alpha particles (helium) and 1% high energy and highly charged ions called HZE particles

(Rask J et al 2008 & ICRP, 2013). HZE particles are ions heavier than alpha particles. They have high charge numbers i.e $Z > 2$ and high kinetic energy (E). Examples of these heavy ions include carbon, iron, and nickel. Although a relatively smaller percentage, HZE particles have high LET, are highly penetrating, have greater ionizing power compared to gamma rays and thus, are capable of inducing greater radiation damage (Cucinotta & Durante 2009).

Gamma radiation and X-rays: are electromagnetic radiation and behave alike. They do not have either mass or charge. They are the residual energy left within a nucleus after radioactive transformation from either alpha or beta decay. They differ in the origin of their emission.

Gamma radiation are high energy photons released from the nucleus while x-rays release from the electron orbital. Gamma radiation is low LET and causes the liberation of low LET electrons when absorbed by matter (indirect ionizing radiation damage) (Keith et al., 1999). Compared to HZE particles, gamma radiation possesses lower penetrating power but also presents as a concerning external radiation hazard (Durante & Cucinotta 2008 and Cucinotta & Durante 2009). Exposures to electromagnetic radiation and charged particles are commonly encountered through medical and occupational exposures. In medical care, cancer radiation therapy utilizes charged particles (carbon and proton) and gamma radiation (gamma knife). Diagnostic medical imaging and interventional procedures utilize x-ray and gamma radiation (Fauci 2018).

BIOLOGICAL EFFECTS OF RADIATION

DNA is the most important target for radiation toxicity (Keith et al., 1999). The type of radiation determines the extent of cellular injury. Direct ionizing radiation interaction with DNA leads to single or double strand DNA breakage and/or base pair damage. In indirect ionizing radiation, damage occurs when radiation ionizes water molecules within and outside the cell

creating free radicals and reactive oxygen species. These agents in turn can act directly on the DNA and other cellular molecules, leading to DNA and macromolecular damages such as single and double strand DNA breakages. A double strand DNA break increases the risk for aberrant DNA repair, consequent cell death, chromosomal aberrations (i.e translocation or deletion) , nondisjunction of homologous chromosomes, introduction of oncogenes during replication, abnormal division in the gonadal cell and potential hereditary disorders (Marci et al 2018, Halperin EC et al., 2018).

In addition, high LET radiation causes complex clustered DNA damage. Cellular radiobiology model studies reveal that when high LET radiation traverses a cell, a dense linear penetrating ionization core track is observed with energetic electrons (delta rays) diffusely emanating and dispersing in multiple directions perpendicularly from the core track (Figure 1a and 1b) (Goodhead, 1994). The higher the energy the longer the distance of the secondary delta rays. However, for an HZE particle of a given charge, the higher intensity, shorter length delta rays seen with lower energy are associated with more clustered DNA damage (Sridharan et al. 2015). One of the biomarkers used in evaluating the biological effects of different radiation qualities is phosphorylated histone 2AX (gamma-H2AX) which is rapidly activated in response to DNA DSBs (Kuo & Yang 2008). Sridharan et al. 2015 found greater induction of phosphorylated H2AX associated with high LET HZE radiation compared to low LET X-rays 2 or 24 hours after exposure. Mishra et al 2017 unexpectedly found the lower LET charged oxygen ions caused greater dose-dependent ovarian DNA damage, oxidative lipid damage, and apoptosis, and greater resultant primordial ovarian follicle depletion in mice compared to higher LET charged iron ions. The authors speculated that this could be due to the greater fluence of the charged oxygen particles.

The harmful health effects of ionizing radiation have been divided into 2 categories: As defined by the National Council on Radiation Protection and Measurements (NCRP),

- a) Deterministic effects: These are dose dependent effects. Adverse tissues damage and physiologic impairment, organ malfunction and death are observed when the threshold dose is exceeded enough to damage a critical number of cells. The health effect can be evident early in the course after exposure, i.e., acute radiation syndrome, or may occur later in life. In the context of repro-toxicity– acute to chronic ovarian dysfunction)
- b) Stochastic effects- This follows the linear no-threshold hypothesis in which DNA damage and chromosomal aberration during replication leads to mutation in somatic cells, resulting in carcinogenesis, or in the germ cell, resulting in hereditary transmission of the mutation to an offspring.

In assessing the reproductive toxicity risks to female astronauts, the premise that HZE particles have greater relative biological effectiveness than gamma radiation with regard to ovarian follicle destruction has been proposed, but not conclusively demonstrated. Mishra et al 2016 & 2017 investigated the ovarian effects of high LET charged iron and oxygen particles in mice. They calculated that the ED₅₀ for primordial follicle depletion was 4.6 cGy for oxygen ions and 27.5 cGy for iron ions at energy of 600 MeV. However, there needs to be a comparison study to determine the ED₅₀ for primordial follicle depletion by gamma radiation using mice of the same strain and age in order to determine the relative biological effectiveness.

We analyzed the dose-response for ovarian primordial, primary and secondary follicle destruction by low dose gamma irradiation from a cesium radioisotope using a mouse model.

We hypothesized that exposure to gamma radiation will cause dose-dependent destruction of

ovarian primordial, primary, and secondary follicles and morphological reduction in ovarian size.

CHAPTER 2: LITERATURE REVIEW

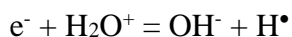
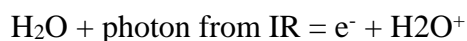
Mechanism of IR Induced DNA Damage and Repair Pathway in Follicular Oocytes

Direct & Indirect Damage of Ionizing Radiation

When healthy cells are exposed to IR, first the physical reaction between the radiation energy and cellular atoms and molecules occurs and then consequentially, cellular dysfunction follows. As mentioned earlier, DNA is the critical target of radiation induced damage. However, in addition to the nucleus, the rest of the cell is also involved in the damage which can lead to the cell death (Keith et al., 1999). This damage can occur either directly or indirect depending the LET of the IR (Hall & Giaccia 2006).

Direct damage involves direct ionization of cellular macromolecules including proteins, DNA and RNA by an ionizing energy resulting in physical and chemical detrimental events that lead to biological damage. This is the mechanism by which high LET charged particle radiation induces damage (Suntharalingam et al., 2005). Indirect cellular damage involves the production of cytotoxic reactive species from secondary effects of ionizing electrons and their interaction with extra molecular components within the cell i.e., water molecules. Water makes up approximately 75-80% chemical composition of a cell. Radiation degradation of water produces cytotoxic compounds namely hydroxyl and hydrogen radicals (Keith et al., 1999; Hall & Giaccia 2006)

Radiolysis of water molecule



The first products of the chemical reaction between IR and water are one highly reactive free electron (e^-) and one positively charged (ionized) water molecule (H_2O^+). The free electron reacts with an available neutral water molecule to form a negatively charged (unstable) water molecule (H_2O^-). Both the H_2O^+ and H_2O^- ions rapidly decompose or react with water to form OH^- ion, and a H^\bullet free radical. The H^\bullet free radical is highly unstable and thus reacts with or ionizes any available macromolecule in its vicinity, including DNA, and disrupts both intercellular and extracellular pH. H^\bullet and OH^\bullet have half-lives of approximately 10^{-11} seconds due to their rapid reaction with DNA and other nearby macromolecules (Keith et al., 1999; Suntharalingam et al., 2005). Radiolysis of one water molecule produces four products; i.e. H^\bullet , OH^\bullet , H^+ and OH^- . The free radical can interact with each other and produce nonreactive molecules like water. Other products of biological consequence include hydrogen peroxide (H_2O_2), hydroperoxy radicals (HO_2^\bullet), hydroperoxy ions (HO_2^-) and reactive nitrogen species (Keith et al., 1999; Pastina & LaVerne 1999). Two thirds of cellular damage caused by ionizing radiation is secondary to indirect effects of free radicals created by ionization of water molecules (Keith et al., 1999). As high LET charged particulate radiation transverses a cell, the generated delta rays (high energy electrons) have low LET and thus cause indirect DNA damage due to ROS generation (Cucinotta & Durante 2009). For example, ^{137}Cs gamma irradiation was measured to generate approximately 60 ROS per nanogram of tissue within less than a microsecond, while a 3.2 MeV alpha particle irradiation generated approximately 2000 ROS which corresponds to ~ 19 nM ROS concentration in the nucleus (Autsavapromporn et al., 2011). Such high nuclear ROS concentration can lead to significant oxidative injury within the cell and disrupt critical biochemical reactions (Sutherland et al., 2000). After IR irradiation the fate of the irradiated cell can be one or more of the following outcomes: a) DNA repair; b) delay

of cellular division and cell cycle; c) adaptation in which the cell develops resistance; d) impaired signal transduction; e) mutation; f) transformation- i.e. carcinogenic transformation of a mutated cell; g) genomic instability; h) apoptosis and cell death (Halperin et al., 2018; Suntharalingam et al., 2005).

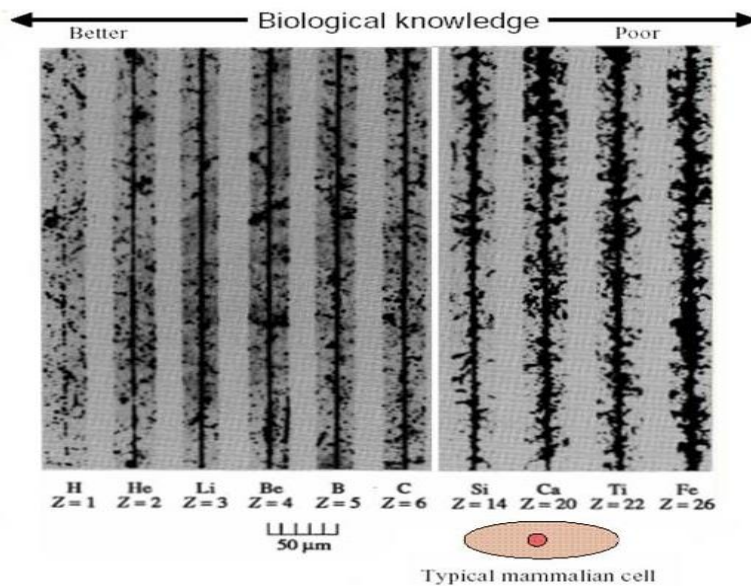


Figure 1a. Comparison of charged particle tracks in nuclear emulsions. The panel shows tracks of different ions, from protons to Fe. One can see the distinction of increasing ionization density ($LET = \Delta E / \Delta x$) along the track as the ion charge Z increases. Taken from Cucinotta and Durante, 2006.

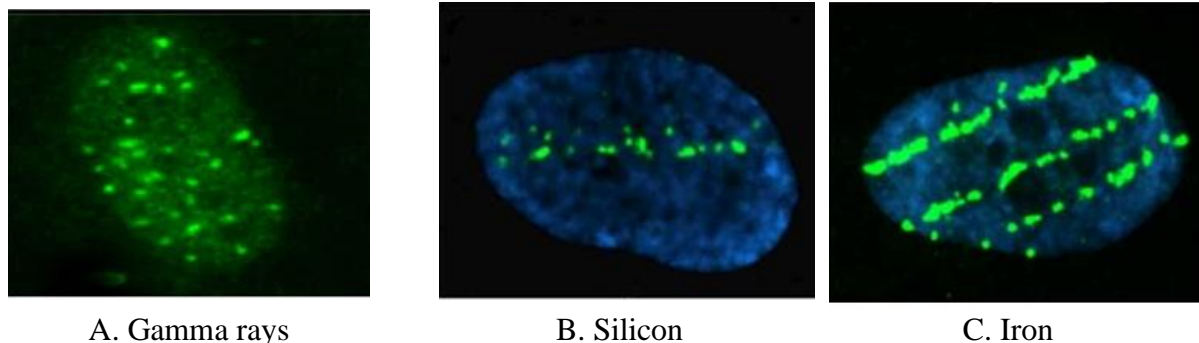


Figure 1b. Comparison of particle tracks in human cell nucleus immunostained for detection of γ -H2AX. The panel shows three nuclei of human fibroblasts exposed to gamma rays (A), Si- (B) and Fe- (C) charged ions. The green florescent focus corresponds to a DNA double strand break (DSB). In the cell exposed to gamma rays (A), one can see uniformly distributed γ -H2AX foci throughout the nucleus. B and C: Exposure to HZE particles shows DNA damage along a linear track in the nucleus (one silicon (Si) and three Iron (Fe) particles). Note: the spacing between DNA double-strand breaks is reduced at a very high LET. Taken from NASA Space Radiation, Cucinotta & Durante 2009

DNA Damage Detection and Repair Pathways

Direct and indirect effects of IR on the DNA results in single strand breaks (SSBs) and double strand breaks (DSBs) through base loss, base changes, breakage of the hydrogen and sugar-phosphate bonds and cross link formation between DNA strands and proteins (Ward 1994; Keith et al., 1999, Sutherland et al., 2000; Pouget et al., 2002). The oocyte like all other cells, is equipped with the ability to detect DNA damage and repair itself at cell cycle checkpoints (see cell cycle checkpoints Figure 2). Replication errors that result when an oocyte is unable to arrest its cell cycle for repair lead to mutations (Kutluk et al., 2015; Stringer et al., 2018).

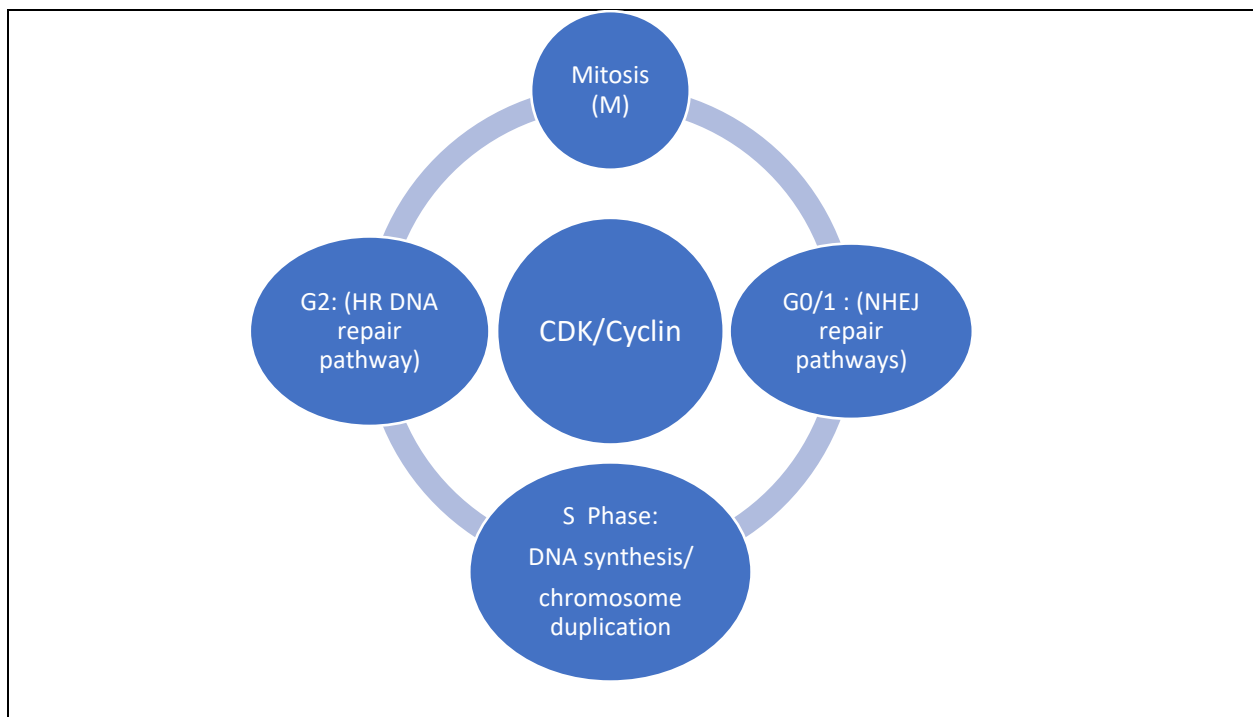


Figure 2: Image of Cell Cycle with checkpoints

The cell cycle is the fundamental process that determines DNA duplication and generation of two daughter cells during cell division.

The cell cycle checkpoints in Gap 1 (G1) and Gap 2 (G2) guard and guarantee that the cycle can proceed to DNA synthesis (S-phase) or mitosis (M). If DNA damage is detected, cell cycle is suspended, and the cell either initiates repair and subsequently continues with the cycle or the cell activates apoptosis and dies. Cell cycle is regulated by various groups of cyclins and cyclin-dependent kinases (CDKs). Cyclin-CDK complexes are involved in the promoting of DNA replication and synthesis. The cell is most sensitive to radiation damage at early S and late G2/M phase of cell cycle

Detection of Radiation-Induced DNA Damage

A spectrum of protein molecules has been implicated in the DNA damage response (DDR) to genotoxic stress. DNA damage is first sensed by Poly(ADP-ribose) polymerase 1 (PARP1) activation, which catalyzes the poly ADP-ribosylation of proteins near the damage site. Subsequent DNA damage sensors are recruited, resulting in loss of PARP1. Single strand breaks are sensed by the 9-1-1 complex of RAD9, RAD1, and HUS1, and double strand breaks are sensed by the MRN complex of MRE11, RAD50 and NBN. Ataxia telangiectasia-mutated (ATM) is recruited by the MRN complex to double strand breaks and ataxia telangiectasia Rad3-related (ATR) is recruited by the 9-1-1 complex to single strand breaks (Valerie & Povirk 2003, Halperin EC et al., 2018). Choudhury et al., 2006 further reported that activation of ATM requires a signaling cascade that includes, telomeric protein TRF2, Rad50, meiotic recombination protein 11 (Mre11), Nijmegen breakage syndrome protein 1 (NBS1), mediator of DNA damage checkpoint protein-1(MDC1) and 53BP1. Activation of ATM leads to the activation of DNA repair proteins and phosphorylation of histone H2AX. Khanna et al., 2001, reported that ATM also plays an important role in the regulation of cell cycle checkpoints namely (S, G1/S and G2/M) after DNA damage. Valerie & Povirk 2003, endorsed that ATM detected IR-induced DSBs in the mammalian cell. Together, ATM, ATR and DNA-dependent protein kinase catalytic subunit (DNA-PKCS) activate p53 and other proteins responsible for DNA repair, delay of cell cycling and apoptosis by phosphorylation (Halperin EC et al., 2018).

DNA Damage Repair Mechanism in oocytes

Two main mechanisms have been identified in the repair of DNA DSBs. Namely non-homologous end joining (NHEJ) and homologous recombination (HR) (Martin JH et al., 2018, Oktay et al 2015 and Collins & Jone 2016).

Homologous Recombination (HR) is the main mechanism for DNA DSBs repair in meiotic cells and hence in both dormant (primordial) and developing oocytes (Kujjo et al., 2010 and Fiorenza et al., 2001). HR plays an important role in the S/G2 checkpoint of the cell cycle (Halperin et al., 2018). HR is a slow and highly reliable mechanism that uses sister chromatids as DNA sequence template.

Mechanism of Homologous Recombination (HR)

DNA DSBs are detected and recognized by the MRN complex which comprises meiotic recombination 11 (MRE11), Rad50-nijmegen breakage syndrome 1 (NBS1). So et al., 2009 found that once the MRN complex binds to the DSB free ends, the NBS1 protein then interacts with ATM dimers causing it to autophosphorylate at serine residues (367, 1893 and 1981). ATM is also attracted to the DNA DSB sites when ATM and the C-terminal region of NBS1 interacts (You et al., 2005). Next, ATM phosphorylates the H2AX histone protein at the C-terminal serine 139 to create γ H2AX. γ H2AX then binds to the DNA damage region and supervises the recruitment of DNA repair proteins (Maidarti et al., 2020). When γ H2AX is phosphorylated, it activates a cascade of events that results in either DNA repair or the arrest of cell cycle (Kutluk et al., 2015). γ H2AX binds to an activated mediator DNA damage checkpoint protein (MDC1), mediated by breast cancer susceptibility gene 1 (BRCA 1). MDC1- γ H2AX complex provides positive feedback loop that further recruits more MRN complexes and γ H2AX propagation at the DNA damage site (Jungmichel & Stucki 2010). It is the activation of ATM (phosphorylation) that determines effective repair of radiation induced DNA damage, initiation of checkpoint kinase 2 for regulation of cell cycle or initiating apoptosis in the case of irreparable damage via activation of TAp63 alpha in oocytes (Maidarti et al., 2020).

NHEJ is comprised of a nuclease, DNA polymerase and ligase which act directly to re-ligate both the upstream and downstream ends of a broken DNA and thereafter rejoins the DNA ends without the use of a sister chromatid as a homologous template. It is identified as an error-prone process and results in either insertion or deletion of base pairs (Lieber MR 2010 and Rodgers & McVey 2016). Other characteristics of NHEJ include a) it can occur independent of the cell cycle (Bekker-Jensen & Mailand 2010) , b) during cell cycling it takes place at the G0/G1 checkpoint , c) NHEJ is most frequently used DNA repair tool in cells undergoing mitosis (Heijink et al., 2013). In oocytes NHEJ takes place in the late stage of oocyte development (Martin et al., 2018).

Mechanism of Non-Homologous End Joining Repair

The pathway occurs in the following sequence- NHEJ repair is activated by a Ku heterodimer named Ku70/Ku80 (aka XRCC6/XRCC5). This polypeptide subunit binds onto each DNA breaks ends and recruits DNA-PKCS which phosphorylates repair proteins including XRCC-4, Artemis, p53 or replication protein (Schulte-Uentrop et al., 2008; Winship et al., 2018). In oocytes, XRCC4 forms a complex with an endonuclease protein Ligase IV to ligate the DSB ends for processing (Winship et al., 2018).

IONIZING RADIATION AND THE FEMALE REPRODUCTIVE TOXICITY

The physical and aeromedical selection criteria for female astronauts are similar to that of male counterparts except for radiation exposure limits and reproductive system. Women can equally participate in space exploration without operational constraint pertaining to gynecological or reproductive health (Jennings et. al. 2000).

Table1. Career Exposure Limits for NASA Astronauts by Age and Gender				
Age (Dose)	25	35	45	55
Female (Sv)	1.00	1.75	2.50	3.00
Male (Sv)	1.50	2.50	3.25	4.00
Sv: Sievert				
Adapted from: NASA Guide Radiation and Human Space Fight 2008				

The career exposure limits for female astronauts (range from 1 to 3 sieverts) are lower than male counterparts (range 1.5 to 4 sieverts) at all ages. Per NCRP this is mainly due to breast and thyroid cancer risk (Jennings et. al. 2000). When compared to a US astronaut, the average dose for any person is 0.0036 Sv, while an individual who works at a nuclear power plant may have an exposure dose of 0.05 Sv. This undeniably shows that astronauts are exposed to significantly higher radiation doses (Table 1).

Table 2. Comparison of various space mission, their duration and observed radiation dose.	
Mission Type	Radiation Dose
Space Shuttle Mission 41-C (8-day mission orbiting the Earth at 460 km)	5.59 mSv
Apollo 14 (9-day mission to the Moon)	11.4 mSv
Skylab 4 (87-day mission orbiting the Earth at 473 km)	178 mSv
ISS Mission (up to 6 months orbiting Earth at 353 km)	160 mSv
Estimated Mars mission (3 years)	1,200 mSv
Adapted from NASA Guide Radiation and Human Space Fight 2008	

Permissible Exposure Limits (PELs)

Table 3. Theoretical Career Effective Dose Limits for 1-year missions based on 3% REID (Average Life-loss for an Exposure-induced Death) for Radiation Carcinogenesis (1 mSv = 0.1 rem)		
	E (mSv) for 3% REID (average life-loss per death [y])	
Age (years)	Females	Males
25	370 (15.9)	520 (15.7)
30	470 (15.7)	620 (15.4)
35	550 (15.3)	720 (15.0)
40	620 (14.7)	800 (14.2)
45	750 (14.0)	950 (13.5)
50	920 (13.2)	1150 (12.5)
55	1120 (12.2)	1470 (11.5)
Adapted from: NASA Human Health and Performance Risks of Space Exploration Missions 2009 & Radiation risk acceptability and limitations. Cucinotta F. 2010.		

An astronaut's career exposure to radiation limit is designed not to exceed 3% due to the risk of exposure-induced death (REID) from fatal cancer (Table 3). These estimations are recommendations obtained from epidemiological data reported by Preston et al., 2003, Cucinotta et al., 2006 and the NCRP 132 report. The estimates of the average life-loss were based on low-LET radiation. It is expected that exposures to high LET from GCR will have higher values.

In literature, tissue targets of radiation induced female reproductive toxicity have been well investigated in female patients who were exposed to ionizing irradiation as part of their

cancer treatments (radiotherapy). They include neuroendocrine dysfunction, uterine toxicity and gonadal ovotoxicity (Agha et al. 2005; The at al. 2014). For example, cranio-spinal irradiation is recommended for treatment in brain cancers and in some hematological malignancies such as Hodgkin's disease. Total body irradiation is oftentimes required before bone marrow transplantation in Hodgkin's disease (Meirow D & Nugent D. 2001). Pelvic irradiation, which is used to treat cervical cancer, endometrial cancer, rectal and bladder cancers, affects both the ovary and uterus (Marci et al., 2018). IR-induced neuroendocrine dysfunction has been associated with disruption of the hypothalamic-pituitary-gonadal axis, as well as growth hormone and gonadotropin deficiencies (Agha et al., 2005). IR exposure damages the uterine endometrium, myometrium and vasculature, causing uterine dysfunction. Ionizing radiation induces ovarian follicular destruction and depletion, with long-term effects that include ovarian insufficiency, premature ovarian failure and subsequent infertility (Teh et al., 2014).

The follicle is the functional unit of the ovary and consists of an oocyte (germ cell) surrounded by supporting somatic cells (granulosa and theca cells). Follicles produce endocrine hormones and are essential for generating mature gametes capable of being fertilized. Therefore, the number of follicles within the ovary is an important predictor of reproductive function. Consequently, external factors such as gamma radiation can accelerate reproductive aging.

Folliculogenesis

Folliculogenesis is a term that describes ovarian follicle growth and development which begins at the reserve of early, quiescent, dormant follicles, called primordial follicle and ends either with ovulation or follicular death by atresia (Figure 3). Growing follicles are categorized

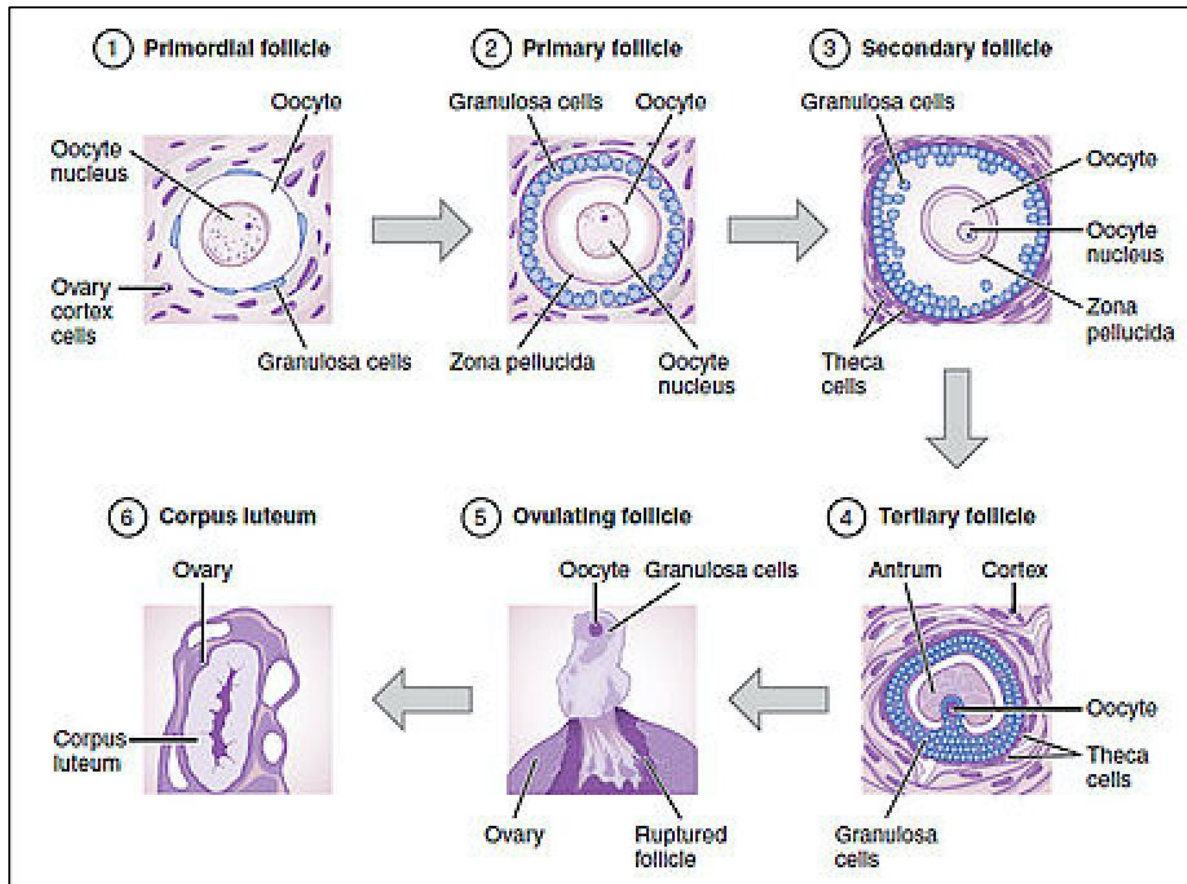
into two morphically different groups- Preantral and Antral follicles. This categorization is based on the presence or absence of a fluid-filled cavity called the antrum.

Preantral follicles include (in chronological developmental order) (i) Primordial, (ii) Primary and (iii) Secondary follicles.

Antral follicles develop into Preovulatory follicles (aka Graafian follicles), which are capable of ovulating an oocyte.

Primordial follicles are dormant follicles which consist of a primary oocyte arrested in first meiotic prophase and surrounded by an incomplete single layer of squamous granulosa cells without basal lamina or zona pellucida (Findlay 2003). Female mammals at birth have a finite abundance of primary oocytes which constitute the ovarian reserve. These follicles can remain dormant for long periods and in the context of astronauts who delay childbirth, up to 40 years. Primary follicles are composed of oocytes surrounded by a complete single layer of cuboidal granulosa cells or mixed squamous and cuboidal granulosa cells outlined by a basal lamina and separated from the oocyte by the zona pellucida. These follicles grow by increasing their oocyte's diameter and increase in number of surrounding granulosa cells. Primary follicles remain in meiotic prophase while undergoing these morphological changes. Secondary follicles are the next developmental stage and are distinguished from primary follicle by their larger diameter, having several layers of surrounding granulosa cells, and a layer of theca cells. Both theca and granulosa cells help in the production of estrogen.

Figure 3: Stages of Folliculogenesis- maturation of an ovarian follicle



[Folliculogenesis](#) by [OpenStax College](#) is licensed under [CC-BY-3.0](#)

The presence of an antrum indicates formation of an antral or tertiary follicle. Its oocyte is surrounded by cumulus cells which are derived from the granulosa cells. Tertiary follicles are larger than secondary follicle and continue to grow in size due to enlarging antrum volume. The last growth and development stage – preovulatory follicles aka graafian follicles are characterized by a larger follicular antrum, eccentrically located oocyte surrounded by the zona pellucid and few layers of granulosa cell which forms a corona called corona radiata.

Surrounding theca and granulosa cells undergo functional changes and develop receptors for FSH and LH. LH induces the production of estradiol in theca cells. FSH induces antral follicles to produce estrogen and inhibin. Both of which in turn regulate FSH release. The oocyte completes the first meiotic division shortly before ovulation. The release of the oocyte from the antral follicle is under the influence of the preovulatory surge of gonadotropin.

Folliculogenesis and regulation of the female reproductive cycle is regulated by the HPG axis through a tightly regulated positive-negative feedback loop involving gonadotropin-releasing hormone (GnRH), luteinizing hormone (LH), follicle-stimulating hormone (FSH) and ovarian hormones (see discussion on HPG axis below). The development of preantral follicles is independent of LH and FSH, while antral follicles development is regulated by LH and FSH. Likewise, estradiol and inhibin hormones produced by antral and preovulatory follicles maintain low levels of FSH and LH. Estradiol provides a negative feedback at the pituitary with a greater effect for LH than FSH (Fauci 2018). Once estradiol production surpasses physiological threshold, this becomes a positive feedback in the hypothalamus leading to upregulation of hypothalamic GnRH secretion, which triggers the preovulatory LH and FSH surges, which trigger ovulation (extrusion of the oocyte from the mature follicle) and luteinization of granulosa and theca cells. This process differs among species, with the surge of GnRH relying on seasonal and/or circadian cues in addition to estradiol positive feedback in some species (Fauci 2018). The remnant ovulated follicle becomes the corpus luteum. The corpus luteum is metabolically active and produces progesterone, which prepares the uterus for implantation in case conception occurs (Hennebold, J. D. 2018).

Effect of Radiation on the Hypothalamic-Pituitary Ovarian (HPO) Axis

The HPO axis is responsible for the complex hormonal regulation required for reproductive maturity, maintenance of ovarian hormone production and folliculogenesis. Secretory neurons in the hypothalamus secrete gonadotropin-releasing hormone (GnRH) in a pulsatile fashion, which stimulates gonadotrope cells in the anterior pituitary to secrete pulses of the gonadotropin hormones luteinizing hormone (LH) and follicle-stimulating hormone (FSH). Both gonadotropins synergistically induce ovarian sex hormone production and folliculogenesis and are also responsible for the initiation of puberty and maintenance of secondary sexual characteristics. The gonads in turn via secretion of sex steroids (estradiol and progesterone in females) and peptide hormones (inhibin) provide feedback regulation of the HPO axis. Therefore, abnormalities in the hypothalamus that decrease GnRH will result in low production of gonadotropins and sex hormones. Likewise, damage to the pituitary that decreases gonadotropin secretion will also result in low production of ovarian sex hormones. Ovarian dysfunction or ovarian failure will result in loss of the negative feedback mechanism resulting in overproduction of gonadotropins. Radiation induced HPO axis dysfunction resulting from either prophylactic or therapeutic cranial irradiation has been associated with multiple hormone deficiencies. Samaan et al. 1982 conducted a retrospective cohort study in which they followed 110 patients, ages 4 - 75 years (70 males and 40 females) for 1 to 26 years after receiving intracranial irradiation for cancer treatment. 83 % were reported to have both physical and biochemical evidence of endocrine deficiency. In females, they found 6 out of 10 who received radiotherapy prior to puberty developed primary amenorrhea in their teenage years, 7 out of 12 women in premenopause (<45 years old) developed secondary amenorrhea, subnormal estradiol,

LH and FSH due to primary pituitary failure 2-5 years after irradiation therapy. Menopausal women (4) who had radiotherapy also developed primary pituitary failure and had no elevation in basal LH and FSH. Patients in this study received a median dose of 50 Gy and 56.2 Gy to the hypothalamus and anterior pituitary, respectively.

Constine et al. 1993 reported primary oligomenorrhea, secondary oligomenorrhea, lower serum estradiol, LH and FSH, hyperprolactemia in postpubertal and premenopausal women who received cranial radiotherapy for brain tumors. In this study the calculated mean radiation dose to the hypothalamus and pituitary gland was 53.6 Gy. Agha et al., 2005 and Marci et al., 2018 reported that radiation induced hypothalamic-pituitary axis dysfunction followed a pattern in which the growth hormone axis is more radiosensitive, followed by gonadotropin, adenocorticotrophic hormone (ACTH) and thyroid stimulating hormone (TSH) axes. Littley et al. 1989 reported in a prospective study that radiation induced neuroendocrine dysfunction is dose dependent. This prospective study included 251 participants, aged between 16-77 years at the time of radiotherapy (X-ray), who had cranial irradiation and whole-body irradiation categorized by radiation dosage (20 Gy, 35-37 Gy, 40 Gy and 42-45Gy). Although Littley et al 1989 did not observe dose-dependent GH deficiency, they however reported universal GH deficiency in all radiotherapy participants. The observed incidences of LH/FSH, ACTH and TSH deficiencies were 85, 78 and 30% respectively in the 35-37.5 Gy dose groups.

The mechanism by which radiation induces HPO axis dysfunction is still under research and poorly understood. However, there are two proposed mechanisms 1) direct cellular injury to the hypothalamus-pituitary cells or 2) via reduced hypothalamic blood flow (Hochberg et al 1983, Robinson et al 2001, Chieng et al 1991 and Robinson et al. 2001).

Ionizing Radiation- Induced Ovarian Toxicity

The ovary's functional unit is the follicle. It is hormonally functional and secretes estrogen to support development of maturing gametes. A female mammal is born with a limited number of primordial follicles which diminishes steadily throughout its lifespan due to normal age-related physiologic changes through recruitment and apoptosis. The hormonally regulated, chronological developmental stages of maturing follicles start with primordial follicle (dormant), and progress to primary, secondary, antral and finally pre-ovulatory follicle, which is capable of releasing its oocyte. A very small percentage of primordial follicles complete the development cycle to reach the pre-ovulatory stage. Both intraovarian and extraovarian factors influence the cyclicity of this development. Younger ovaries have larger total number of ovarian follicles than older ovaries (Gosden et al., 1983). Follicular atresia is hormonally controlled, and part of a regulatory mechanism designed to manage the number of ovarian follicles selected for ovulation (Hirshfield 1988 & 1997). Factors that affect the reproductive toxicity of radiation include age, field of irradiation, type of radiation, dose and duration of radiation exposure (Munoz et al. 2016). Advances in the study of radiation induced reproductive toxicity comes from epidemiological studies of radiation nuclear disasters (Chernobyl, Hiroshima and Nagasaki nuclear bombs), accident occupational exposures, radiotherapy in cancer patients, experimental animal models, and in vitro studies.

The radiation dose required to destroy half of immature oocytes in women is estimated to be less than 2 Gy (Marci et al. 2018; Wallace et al., 2003), while 25-50 Gy could cause infertility in one-third of young women and almost all over the age of 40 (Marci et al. 2018). Temporary amenorrhea and premature ovarian failure are reported complications of therapeutic electromagnetic radiation (Wallace et al. 1989, Meirow & Nugent 2001, Lo Presti et al. 2004).

Experimental animal studies have helped to provide mechanistic explanation of the potential pathway and cellular components involved in radiation induced cellular toxicity and repair mechanisms.

The ovary is highly sensitive to gamma-radiation. Dormant primordial follicles have been identified to be most radiosensitive to gamma radiation (Kim & Lee 2000). Although, gamma radiation destroys follicles at all stages of growth, Lee et al., 2000 showed that gamma radiation induced apoptotic degeneration and morphological follicular degeneration in primordial and primary follicles in prepubertal mice ovaries. However, primordial follicular degeneration occurred much faster than observed in primary follicles. Lee and Yoon, 2005 observed that prepubertal female mice irradiated with gamma radiation showed higher frequency of atretic antral and preantral follicles after 2 and 3 days after irradiation. They also found that in addition to apoptotic degeneration, macrophages were phagocytosing neutrophils in the follicular cavity thus signifying activation of the inflammatory immune response.

The precise cellular and molecular mechanism of radiation induced follicular damage is still under continuous scientific investigation. However, some experimental studies have shown the mechanism of action of gamma radiation induce repro-toxicity involves production and prolonged elevation of cellular ROS and oxidative stress and consequent ROS induced apoptosis of ovarian follicles (Cortes-Wanstreet et al., 2009).

Hanoux et al., 2007 demonstrated the genotoxic stress caused by gamma radiation triggers a mitochondrial pathway of apoptosis via early activation of Caspase 2 and sequential activation of caspase -9 and 3. The author suggested that oocyte radiosensitivity of preantral and antral follicles may be dependent on the expression of pro and anti-apoptotic regulators. They found that quiescent oocytes of primordial follicles have stronger expression of caspase 2

compared to growing follicles. Livera et al., 2008 identified that transcription factor 63 alpha (TAP63 α) is phosphorylated after gamma radiation-induced DNA damage thus inducing apoptosis in primordial oocytes. Kerr et al., 2012 reported a mechanism that involved proapoptotic proteins BAX and BAK. They demonstrated that DNA damage by gamma radiation activated TAP63 α which induces p53 upregulated modulator of apoptosis (PUMA) and p53-inducible gene (NOXA). These proteins bind and inhibit pro-survival B-cell lymphoma 2 (Bcl2) group of proteins activity (an anti-apoptotic protein implicated in repairing mitochondrial permeability), and PUMA activates proapoptotic protein B-cell lymphoma (Bcl)-associated X (BAX) (located in cytosol) and Proapoptotic B-cell lymphoma 2 antagonist/killer (BAK) (located in mitochondrial membrane) which leads to apoptotic cell death. The authors showed by blocking PUMA and NOXA that the ovarian reserve was preserved from cell death by apoptosis.

Radiation Induced Uterine Damage

The uterus is a hollow, muscular organ located in the mid hypogastric region of the abdomen located between the bladder and rectum. It is composed of two parts- the corpus (upper two-thirds) and cervix (lower one-third), which have different embryonic origins. The uterus has three tissue layers, namely: the inner endometrium (mucous membrane), middle serous, and outer myometrium (muscular membrane). In premenopause, the endometrium undergoes three unique phases – proliferative, secretory and menstrual phases. Histologically, the uterus is lined by ciliated simple columnar epithelium (endometrium), columnar and squamous epithelium (cervix), and secretory columnar epithelium (endocervix). During the follicular phase of the ovarian cycle, the preovulatory rising concentration of estradiol is responsible for proliferative changes in the endometrium (Grigsby et al., 1995). In the presence of estrogen, cellular

proliferation, maturation and desquamation of the uterus takes place. During the luteal phase, both estrogen and progesterone are responsible for the secretory changes that occur in the endometrium should implantation occurs. If implantation does not occur this leads to a progressive decline in hormonal stimulation of the endometrium. The absence of estrogen stimulation causes atrophy of the uterine smooth muscle and endometrial mucosa, as well as ischemic vascular changes which lead to release of cytokines, cell death and shedding of the endometrium (Fauci 2018). Likewise, during menopause, estrogen concentration is significantly reduced, which consequently leads to reduction in the uterine weight and size.

The average age of female astronaut-candidate finalists is 32 and their average age at first space flight is 38 (Jennings et al., 2000). Pregnancy during astronaut training and or planned future space flight leads to aeromedical grounding or disqualification. Therefore, it is not uncommon to find prevalent use of contraception amongst female astronauts. Female astronauts safely use combined estrogen and progestin oral contraceptive pill to suspend their menstrual periods during space travels (Jennings et al., 2000). Studies that investigated radiation induced uterine effects in female patients who received total body or abdominal radiation therapy (20 – 30 Gy) and abdomen during childhood reported adult-onset reproductive problems including uterine dysfunction due to impaired uterus development, reduced uterine size and impaired uterine blood flow (Critchley et al., 1992; Bath et al., 1999; Holm et al., 1999, Larsen et al., 2004). All three studies used doppler ultrasonography measurements to measure uterine length, volume and vasculature. Both Critchley et al., 1992 and Larsen et al., 2004 concluded that the radiation dose of > 25 Gy to the uterus during childhood likely induced an irreversible damage. Studies that investigated radiation induced uterine outcomes in adult women, reported that exposure to total body irradiation of 12 Gy is associated with greater risk of miscarriage, pre-

term labor and low birth weight infants (Teh et al., 2014). Compared to the ovary, the radiation dose threshold for complete uterine dysfunction to occur such that pregnancy is unsustainable is unknown. In the literature, no successful term pregnancy has been published after direct pelvis irradiation of > 45 Gy (Teh et al., 2014). Histological findings after high dose uterine irradiation include lipid-containing foamy histiocytes in the endometrium, ulceration, coagulative necrosis, post healing dense collagen scar, atypical fibroblast and rare glands with atypical nuclei and telangiectatic blood vessels. Myometrium changes include vascular damage due extensive arteriolar myointimal proliferation and arteriosclerosis and cervical atrophy (Grigsby et al. 1995).

CHAPTER 3: METHODOLOGY

Animals

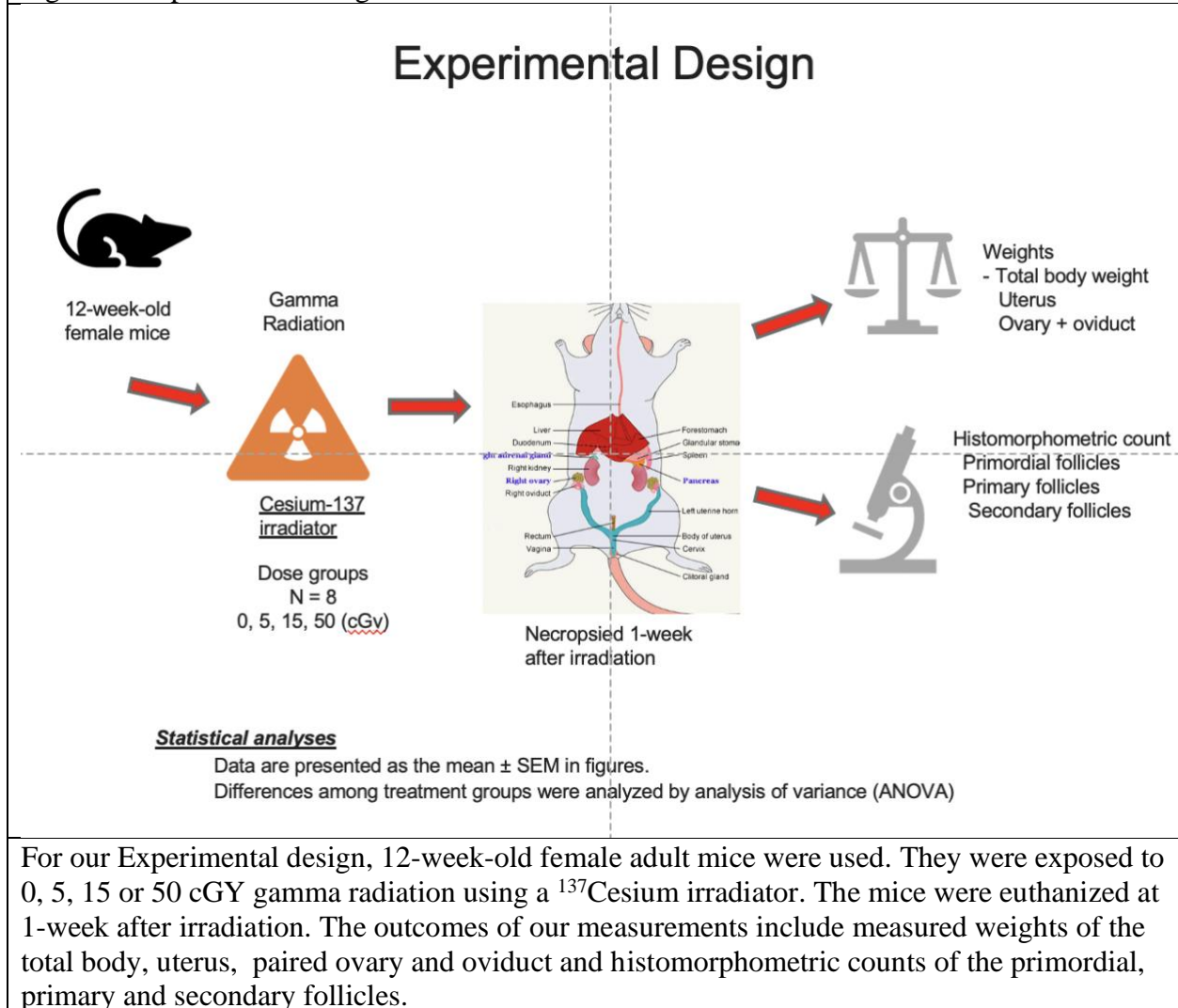
Eleven-week-old female C57BL/6J mice were purchased from Jackson Labs and were allowed to acclimate for one week prior to irradiation. The mice were housed in an American Association for the Accreditation of Laboratory Animal Care Facilities International (AAALACI)-accredited vivarium with a 12h/12h light/dark cycle, with controlled temperature and humidity. The mice had ad libitum access to regular chow until euthanasia. All animal procedures were approved by the Institutional Animal Care and Use Committee at University of California Irvine.

Experimental Design

Mice (n= 8/experimental group) were exposed to 0, 5, 15 or 50 cGy gamma radiation using a Cs137 irradiator at dose rates of 13.5–18.6 cGy/min. Mice for the 0 cGy group were transported and restrained identically to the irradiated groups. Irradiations were performed at the UCI Department of Radiation Oncology irradiation facility CA, USA.

Mice were euthanized by CO₂ inhalation at 1 week after irradiation. Body weight was measured, and ovaries, uteri, and blood were collected at the time of euthanasia. Ovaries and uteri were weighed prior to processing.

Figure 4: Experimental design



Ovarian histomorphometric analysis

One ovary was fixed in Bouin's fixative for 24 hours at 4°C, washed in 50% ethanol four times, and stored in 70% ethanol until embedding in paraffin. Our laboratory placed 4 or 5 ovaries and a piece of uterus each in one chamber of a 6-chambered cassette before the cassettes were sent to the Pathology Core Facility, where they were embedded in paraffin in the same order and pattern as in the 6-chambered cassette. The paraffin blocks containing ovaries and uterus were then serially sectioned at 5 µm thickness all the way through the entire tissue. Sections were stained

with hematoxylin and eosin for histopathological examination blinded to the experimental group by a board-certified veterinary pathologist. The other ovary from each mouse was fixed in 4% paraformaldehyde in PBS and cryoprotected in 30% sucrose in PBS prior to being embedded in OCT for immunostaining. Immunostaining data are not part of this thesis. Complete serial histologic sections from each ovary were evaluated by one of the investigators (O. Awodele) without knowledge of genotype or treatment using an Olympus BX60 light microscope equipped with Plan Fluor x10, x20, and x40 objectives, and Plan Achromat x4 objective (Olympus America). Ovarian follicles were classified as primordial (oocytes with single layer of flattened granulosa cells), primary (oocytes with single layer of cuboidal or mixed cuboidal/flattened granulosa cells), or secondary (oocytes with more than one layer of granulosa cells) as described previously (Lopez and Luderer, 2004; Lim et al., 2013) (Figure 8) . Primordial, primary and secondary follicles were counted in every fifth serial section. The counts were multiplied five times to obtain estimates of the total number of follicles per ovary. To avoid overcounting, primordial and small primary follicles were only counted if the oocyte nucleus was clearly visible, and larger primary and secondary follicles were only counted if the oocyte nucleolus was clearly visible (Canning et al., 2002).

Statistical analyses

All data are presented as the mean \pm S.E.M in figures. For the measured weight outcomes, Shapiro-Wilk test was used to test whether the variables were normally distributed. Differences among treatment groups for both measured weight outcomes and histomorphometric counts were analyzed by analysis of variance (ANOVA). For follicle count data, if the result of one- way ANOVA indicated that there was a statistically significant difference in the means of the follicle

count ($p\text{-value} < 0.05$) among the 4 dose groups, then the multiple comparisons (pair-wise comparisons) method was performed. The reason to perform the pairwise comparisons method is to study which 2 groups are statistically significant different in the means of the follicle counts. Bartlett's and Levene's tests were used to test for equality of variances for follicle counts. Differences among dose groups were also analyzed by non-parametric Kruskal–Wallis test followed by Mann–Whitney U test for intergroup comparisons because the normality assumption was not met for some of the data analyzed. The non-parametric Kruskal–Wallis test will indicate whether there is a statistically significant difference in the distributions of the outcome variable (ie. primordial, primary or secondary follicles) among the 4 dose groups. If the result of Kruskal–Wallis test indicated that there is a statistically significant difference ($p\text{-value} < 0.05$), then the Dunn's test (of multiple comparisons using rank sums) method will be performed. P- value was set at 0.05 to indicate statistical significance. Statistical analyses were carried out using STATA IC app.

CHAPTER 4: RESULTS

Part 1: Total Body Gamma Radiation Effects on Measured Weight Outcomes

To test whether each variable was normally distributed, Shapiro-Wilk test (p value 0.05) was used. The p-values for wet uterus and paired ovary+oviduct were <0.05 indicating that the data were not normally distributed. A logarithmic (base 10) transformation was therefore used in order to achieve normality. ANOVA was used to test whether the means of the weight variables are the same among the four gamma radiation doses (Table 4).

Overall, there was statically significant effect of gamma radiation dose on the measured total body weights amongst dose groups (P=0.04). Specifically, the weights in the 5 and 15 cGy dose groups were significantly lower than controls. We observed no statistically significant association between gamma radiation doses and wet uterus weights (p-value = 0.49) or ovarian weights (P=0.23). See Figures 4-7 below.

Table 4: Summary statistics, Gamma ray dose vs. measured variables (total body weight, wet uterus and paired ovary + oviduct)							
Gamma ray dose	n	Total body weight ^a		Wet uterus		Paired Uterus +Oviduct	
(cGy)	Total: 32	Mean (g)	SD	Mean (mg)	SD	Mean (mg)	SD
0	8	20.17	0.96	95.25	24.02	14.2	2.28
5	8	19.07 ^b	0.84	72.96	18.21	13.11	1.39
15	8	19.24 ^c	0.61	81.23	39.36	12.89	0.82
50	8	19.70	0.66	83.03	41.22	12.39	2.09

n: number of ovaries

SD: standard deviation

^a P=0.04, one-way ANOVA for total body weight mean difference

^b P=0.009 versus 0 cGy by Dunn's test for pairwise comparisons

^c P=0.025 versus 0 cGy by Dunn's test for pairwise comparisons

Effects of gamma irradiation on total body weight, wet uterus and paired ovary+oviduct weights (mean \pm std dev) of 12-week-old female C57BL/6J mice one week. Mice were euthanized by CO₂ inhalation at 1 week after irradiation. One-way ANOVA and Dunn's test (for pair wise comparison) for 5 and 15 cGy gamma radiation dose group for total body weight showed statistical significance $p < 0.05$.

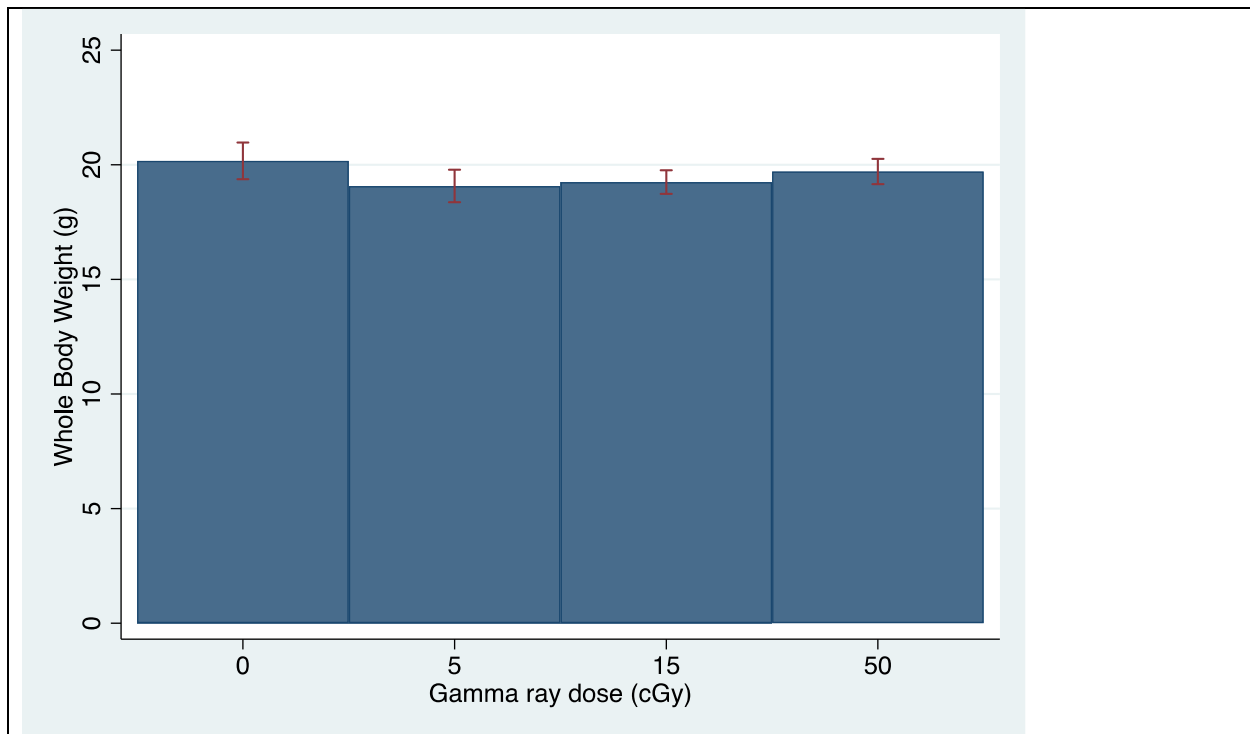


Figure 5: Effects of gamma irradiation on whole body weight (mean \pm std dev) of 12-week-old female C57BL/6J mice one week. Mice were euthanized by CO₂ inhalation at 1 week after

irradiation. Whole body weights were measured before euthanasia. Gamma irradiation caused statistically significant reduction in body weight. $p=0.0397$

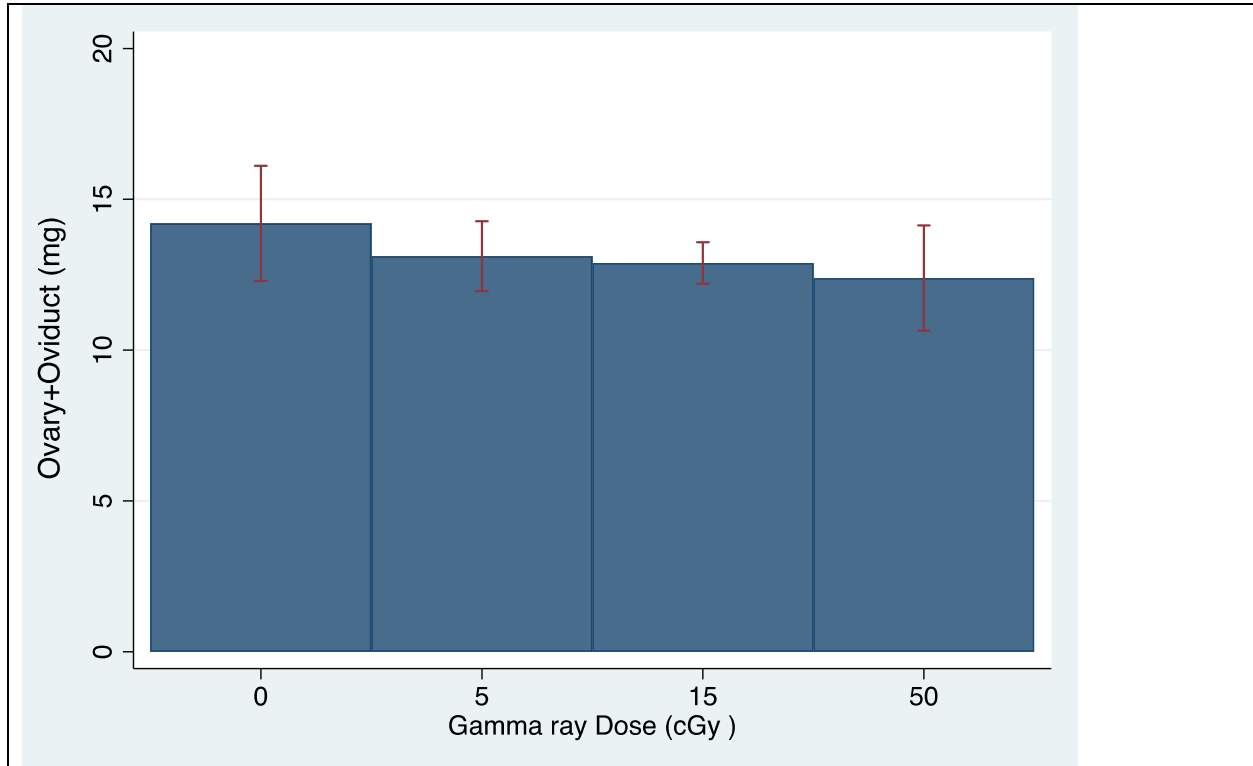


Figure 6: Effects of gamma irradiation on measured weight of paired ovary+oviduct (mean \pm std dev) of 12-week old female C57BL/6J mice one week. Mice were euthanized by CO₂ inhalation at 1 week after irradiation. Paired ovary+oviduct weights were measured after euthanasia. Graph shows gamma irradiation caused non-statistically significant dose dependent reduction in paired ovary+oviduct weight. $p=0.2305$

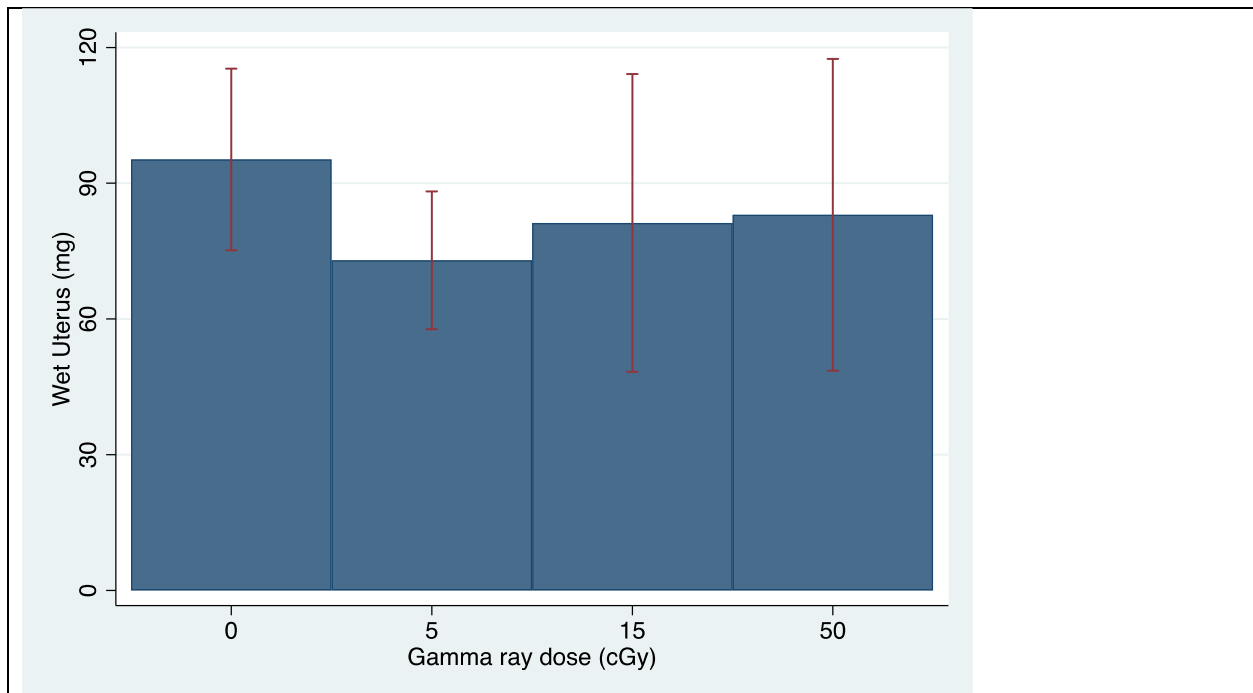


Figure 7: Effects of gamma irradiation on measured wet uterus (mean \pm std dev) of 12-week old female C57BL/6J mice one week. Mice were euthanized by CO₂ inhalation at 1 week after irradiation. Wet uterus weights were measured after euthanasia. Gamma irradiation did not cause statistically significant reduction in wet uterus weight. $p = 0.4917$

Part 2: Histomorphometric counts

The data presented here are only for 3-4 ovaries per group. Counts have not been completed for the remaining 4-5 ovaries per group.

First, we used one-way ANOVA to study whether there is a statistically significant difference in the means of the follicle counts among the different dose groups (i.e. 0, 5, 15, 50 cGy). Our rationale was that if the result of ANOVA indicates that there is statistically significant difference in the means of the follicle counts (i.e., $p\text{-value} < 0.05$), then a multiple comparisons (pair-wise comparisons) method will be performed with the multiple comparisons adjustment applied on the p -values. The purpose to perform the pairwise comparisons method is



to study which two dose groups are statistically significantly different in the means of their follicle counts. Since the data were not normally distributed, we also utilized a non-parametric Kruskal Wallis test to compare means among groups.

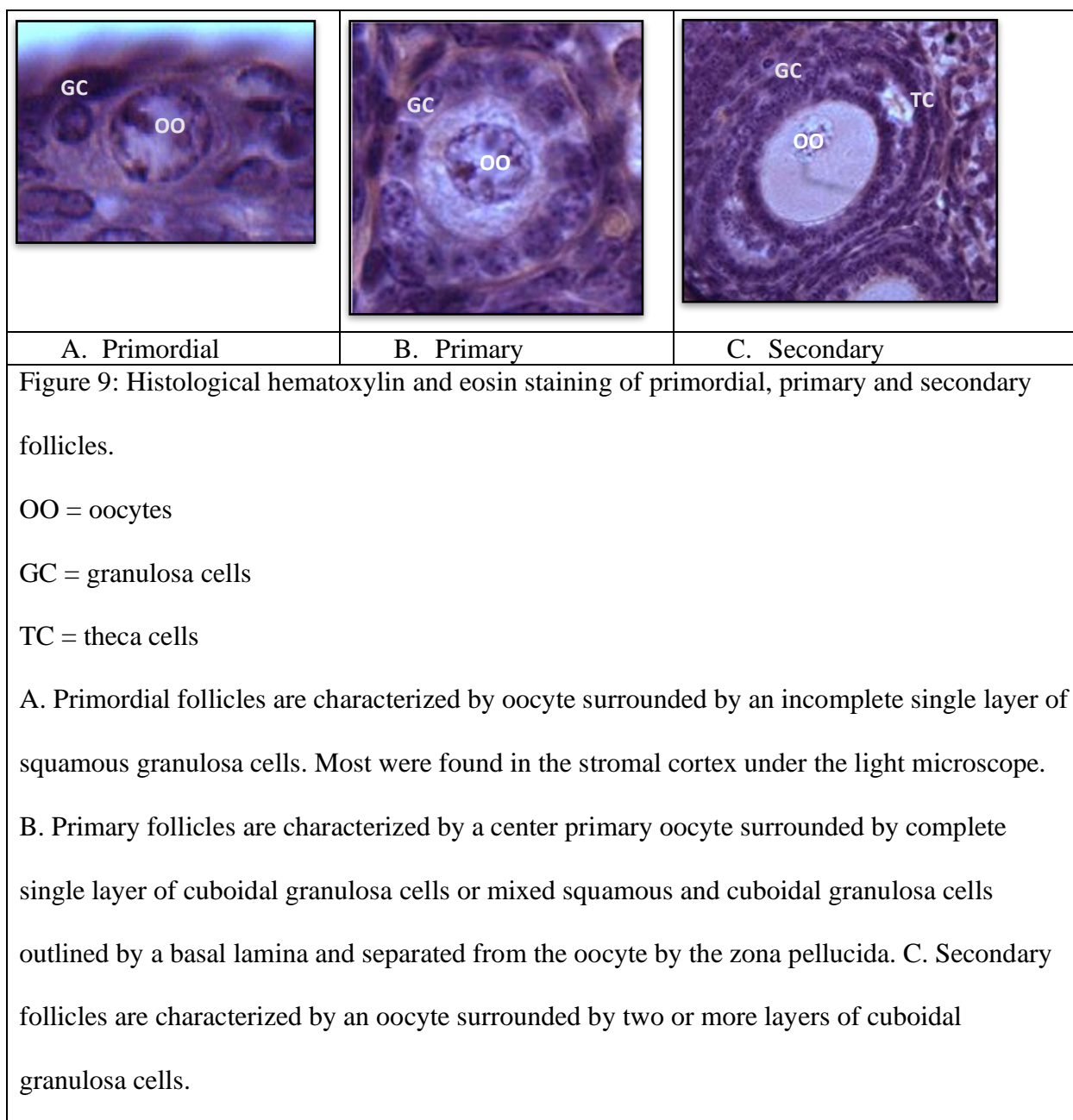
After unmasking the data, we quickly discovered a highly probable error during early initial analysis of the data. Initial results showed that the mean \pm SD of total count of primordial follicles in mice exposed to 50 cGy (476.7 ± 423.6) was close in range with non-irradiated (0 cGy) control mice (470 ± 368). These findings were inconsistent with published data. Pesty et al., 2010 reported drastic destruction of primordial follicles at <24hrs after exposure to 50 cGy gamma radiation and a relative reduction in primary follicle counts as well. Mathur et al., 1991 reported approximately 79%, 87% and 75% follicular depletion in Swiss albino mice ages 1 week, 3 weeks and 6 weeks respectively at 1 day after exposure to 60 cGy of gamma radiation. As described in the methods, our laboratory placed ovaries and a uterus each in one chamber of a 6-chambered cassette as indicated in the figure 12 below. The cassettes were sent to the Pathology Core Facility. A pathology technician embedded the ovaries in paraffin wax in the same arrangement as they were placed in the cassette. The technician then serially sectioned the paraffin block containing the ovaries and piece of uterus onto microscope slides. The masked ovary microscope slide arrangement should have the ovaries arranged identically to the cassette map that our laboratory provided.

We suspect there are 2 possible sources of error that that may have occurred. 1) that the positions of two adjacent ovaries were switched between the cassette and the embedding mold by the pathology technician or 2) our laboratory placed misplaced an ovary in the wrong cassette arrangement. We suspect option 2 less likely occurred because each cassette arrangement was meticulously double-checked when placing the ovaries into the cassettes.

As a result, we re-arranged the positions of ovaries such that the positions of ovaries GG13 with GG2 in cassette 1 and ovaries G6 and GG1 in cassette 3 were switched. (See the figure 12 below for pictographic illustration of our rearrangements).

We present the results of two versions of data analysis. Version 1 data represents data obtained from the un-rearranged histomorphometric counts of primordial, primary and secondary follicles while version 2 data represent data from the re-arranged follicular counts.

Figure 8: Pictographic illustration of ovary rearrangements after discovery of highly probable pathology error.										
Cassett e #	Pathology Cassette Map (Mouse ID)			Postulated masked ovary- slide arrangement			Unmasked Re-arrangement			
1	1	2	3	GG2 [‡]	G8	G15		GG13	G8	G15
	GG13	G8	G15	GG13	GG15	UT GG15		GG2 [‡]	GG15	UT GG15
	4	5	6							
	GG2*	GG15	UT GG15							
2	1	2	3	G7	GG4 [‡]	G16		G7	GG4 [‡]	G16
	G7	GG4*	G16	G5	GG14	UT G8		G5	GG14	UT G8
	4	5	6							
	G5	GG14	UT G8							
3	1	2	3	GG1 [‡]	GG1 6	G13		G6	GG16	G13
	G6	GG16	G13	G6	G14	UT G14		GG1 [‡]	G14	UT G14
	4	5	6							
	GG1*	G14	UT G14							
<p>* = Ovary exposed to highest dose (50 cGy)</p> <p>‡ = Ovary with lowest follicular count</p> <p>UT = Uterus</p> <p>Note: Cassette # 2 did not require rearrangement.</p>										



VERSION 1 DATA RESULT:

Overall, there were more primordial follicles counted than primary follicles which was more than secondary follicles (Table 6). The effect of gamma irradiation on follicular count showed no statistical significance for primordial, primary and secondary follicles (p-value > 0.05). One way ANOVA and Kruskal Wallis tests were used to determine if there is a

statistically significant difference in the means of the follicle counts among the different dose group. The F-statistics and P-values from the ANOVAs for primordial, primary and secondary follicle counts were $F=0.37$, $p= 0.7740$; $F=1.12$, $p= 0.3811$; and $F= 0.43$, $p= 0.7331$, respectively (Figure 8-10). Both Bartlett's test and Levene's test showed that the equal variances assumption amongst dose groups was met. A Kruskal-Wallis equality of populations rank test was conducted to determine if the follicle counts differed among the four dose groups. Kruskal-Wallis test, like the ANOVA, showed that there was no statistically significant difference between the four dose groups in the primordial follicle count ($\chi^2 = 2.079$, $p = 0.5561$), primary follicle count ($\chi^2 = 2.465$, $p = 0.4817$) and secondary follicle count ($\chi^2 = 1.465$, $p = 0.6905$).

Table 5: Summary data of follicle count per gamma dose exposure.									
Dose (cGy)	Primordial			Primary			Secondary		
	Mean	SD	SEM	Mean	SD	SEM	Mean	SD	SEM
0	470	367.9	183.9	166.3	177.7	88.8	150	69.4	34.7
5	348.8	325.1	162.5	122.5	123.1	61.5	118.8	44.8	22.4
15	618.8	344.2	172.1	322.5	208.7	104.3	163.8	76.6	38.3
50	476.7	423.6	244.6	155	134.3	77.5	116.7	81.1	46.9
Number of counted ovaries = 15, N=4/group, except for 50 cGy N=3.									
SD: Standard Deviation									
SEM: Standard Error of Mean									

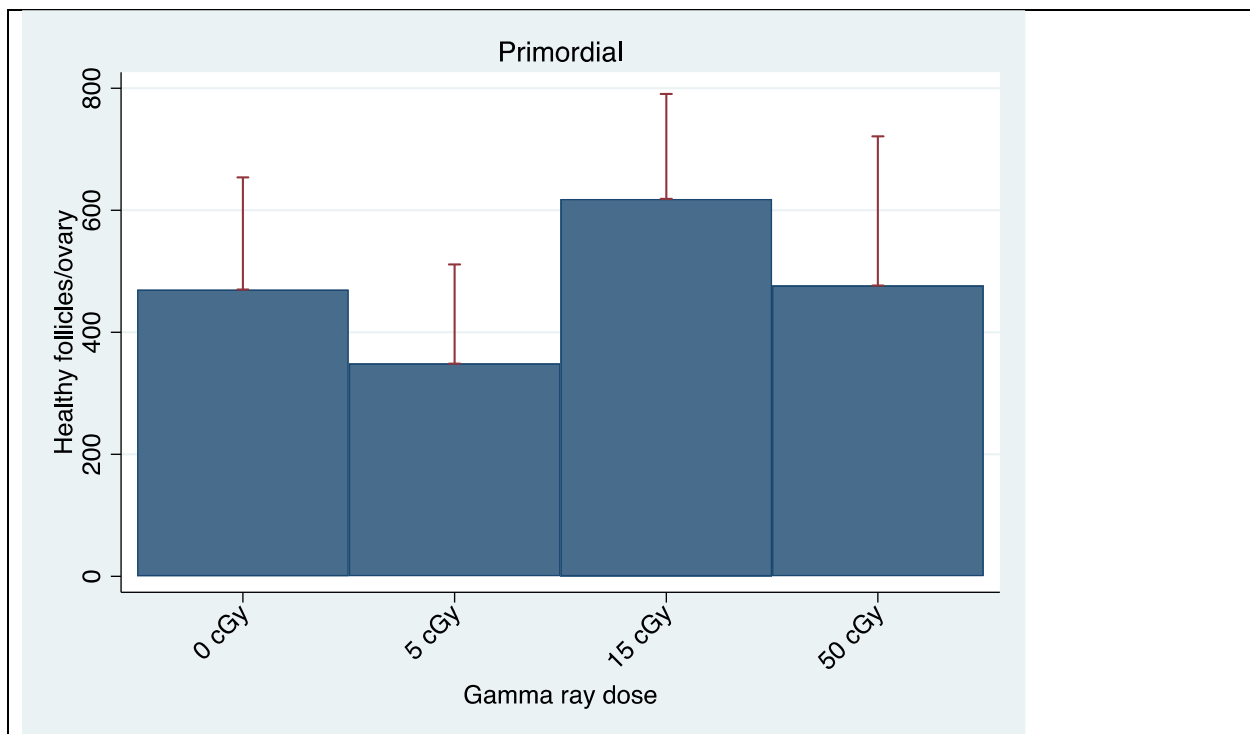


Figure 10. Figure 3. Primordial follicles count. N = 3-4 mice/dose group. Graphs shows the mean \pm S.E.M. of numbers of healthy primordial follicles 1 week after exposure to varying doses of gamma irradiation. There is no statistically significant difference in the means of the follicle counts among the different dose groups ANOVA; $p = 0.7740$.

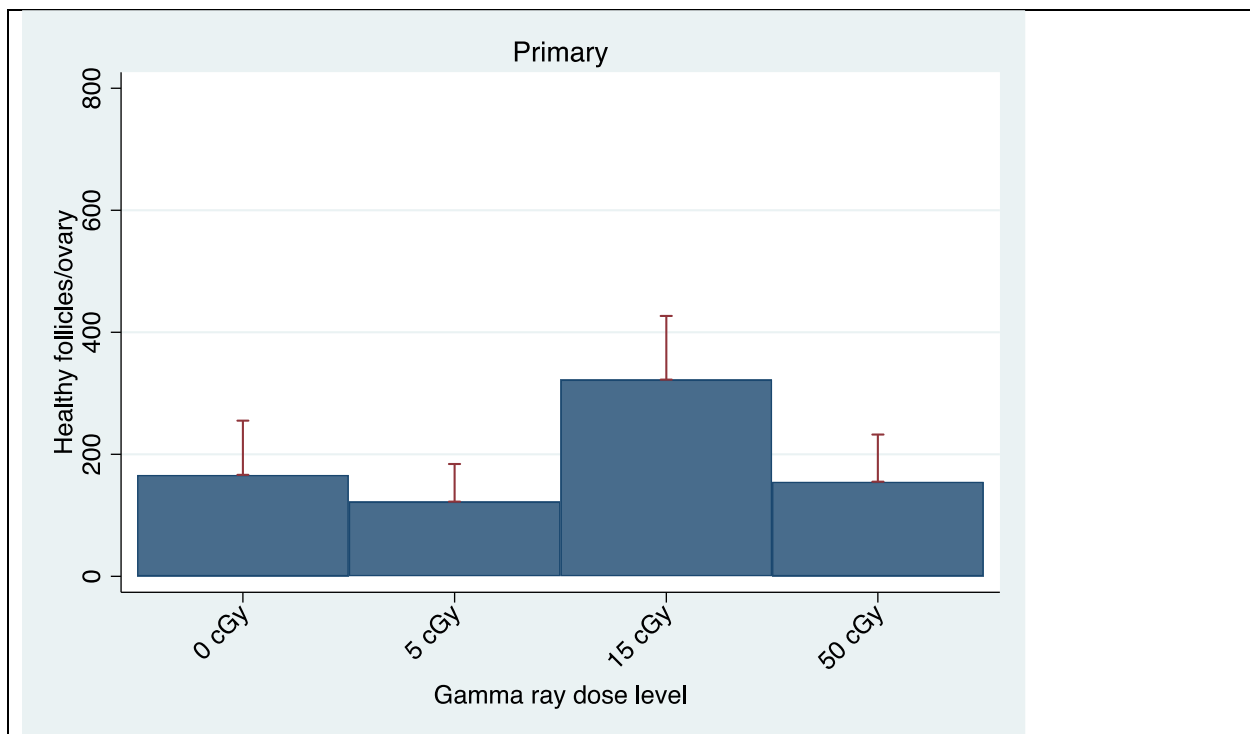


Figure 11. Primary follicles count. N = 3-4 mice/dose group. Graphs shows the mean \pm S.E.M. of number healthy primary follicles 1 week after varying doses of gamma irradiation. Gamma irradiation did not cause statistically significant depletion of primary ovarian follicles. On the contrary, the graph shows inconsistent relationship of follicle count and dosages of gamma irradiation. The difference in the means of the follicle counts among the different dose groups did not show statistically significance ANOVA; $p = 0.3811$.

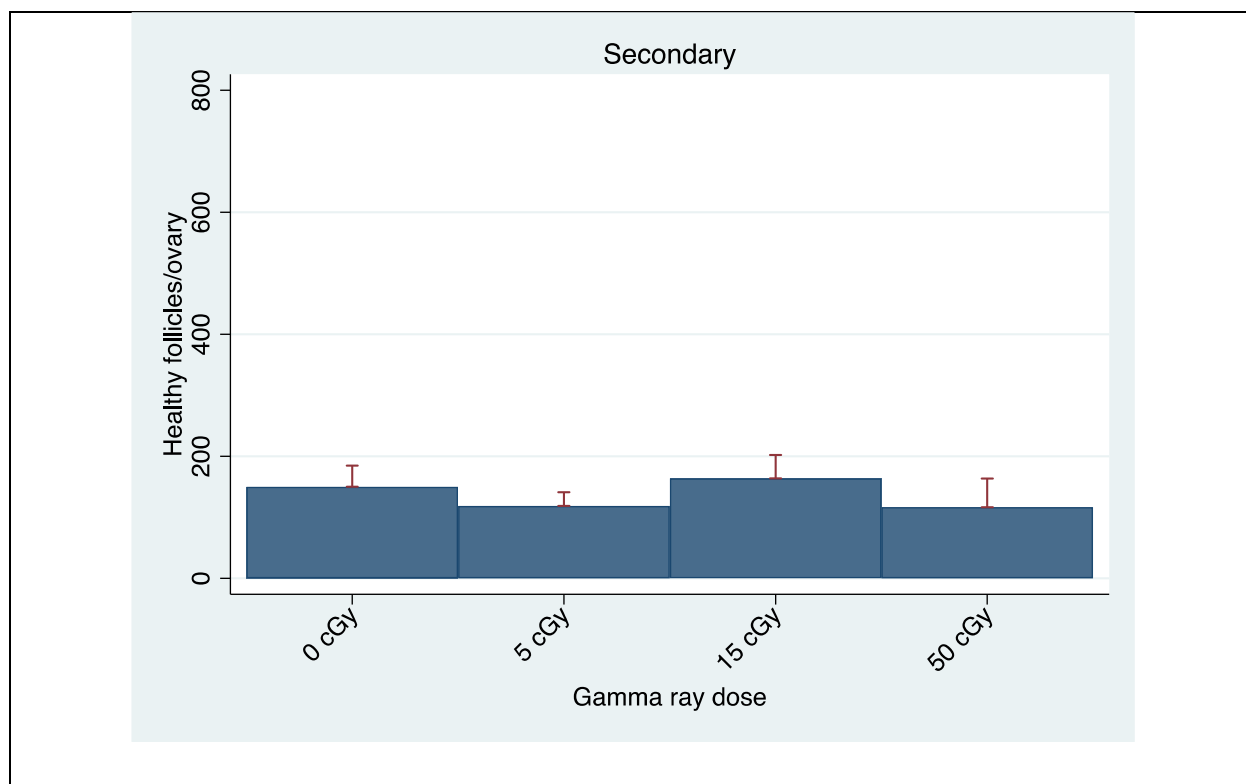


Figure 12. Secondary follicles count. N = 3-4 mice/dose group. Graphs shows the mean \pm S.E.M. of number healthy primordial follicles 1 week after varying doses of gamma irradiation. Higher dose gamma irradiation did not cause statistically significant depletion of secondary ovarian follicles. On the contrary, the graph shows inconsistent relationship of follicle count and dosages of gamma irradiation. The difference in the means of the follicle counts among the different dose groups did not show statistically significance ANOVA; P = 0.7331.

VERSION 2 DATA RESULT (Rearranged ovary cassette map).

Overall, there were more primordial follicles counted than primary follicles, and there were more primary than secondary follicles (Table 7).

One-way ANOVA was used to determine if there were statistically significant differences in the means of the follicle counts among the different dose groups (i.e., 0, 5, 15, 50 cGy) for

primordial, primary and secondary follicle counts were ($F=4.98$, $p= 0.0202$; $F=3.08$, $p= 0.0722$; and $F= 2.55$, $p= 0.1095$) respectively. Only primordial follicle numbers showed statistically significant differences in the means of the different dose groups.

The mean \pm S.E.M. of number healthy primordial follicles 1 week after gamma irradiation showed a dose dependent depletion of primordial follicles with increasing dose concentration. 15 cGy gamma irradiation caused an increase in number of healthy follicles counted compared to 5 cGy (Figure 13). However, this increased count was not statistically significant after pairwise comparisons of marginal linear predictions and after Mann-Whitney rank-sum test ($p= 0.8845$ and 0.2482 respectively). 50cGy gamma radiation caused statistically significant complete total destruction of primordial follicles 1-week after irradiation. Both Bartlett's test and Levene's test show that the equal variances assumption was met. After intergroup comparison amongst the three dose groups compared to the control group (0 cGy) for primordial follicles count, we can only reject the null hypothesis that the variances are equal for the 50cGy dose group (p -values < 0.05). Pairwise comparisons of marginal linear predictions for primordial follicle count 1-week after exposure to 50 cGy gamma irradiation showed statistical significance [50 vs 0 (cGy): $p= 0.005$, 95% Conf. Interval (-1085.1, -254.1); 50 vs 15 (cGy): $p= 0.007$, 95% CI (-1032.6, -201.6) and 50 vs 5 (cGy): $p= 0.022$, 95% CI (-917.6, -86.6)]. The purpose to perform the pairwise comparisons method is to study which two dose groups are statistically significantly different in the means of their follicle counts. Kruskal-Wallis test showed that there was statistically significant difference between the four dose groups in the primordial follicle count only ($\chi^2 = 7.985$, $p = 0.0463$), while both primary follicle count and secondary follicle count did not show statistical significance $\chi^2 = 7.398$, $p = 0.0602$; $\chi^2 = 6.836$, $p = 0.0773$ respectively. Wilcoxon-Mann-Whitney rank-sum test was conducted to determine if

changes in follicle counts due to gamma radiation was different for the three dose groups compared to the control group (i.e., 0 cGy). Wilcoxon-Mann-Whitney rank-sum test showed that there was statistically significant difference in primordial follicle count between the 50 cGy gamma radiation doses when compared to no radiation.

Gamma irradiation apparently caused depletion of primary ovarian follicles. However, the difference in the means of the follicle counts among the different dose groups approached, but did not attain statistical significance (one-way ANOVA; $p = 0.0722$). Increasing dose of gamma radiation showed a pattern of dose dependent depletion of primary follicles except for 15 cGy dose. 50cGy gamma radiation caused complete total destruction of primary follicles 1-week after irradiation (Figure 14). Similarly, gamma irradiation apparently caused 59% depletion of secondary ovarian follicles 1 week after gamma irradiation; however, this was not statistically significant (one-way ANOVA; $p = 0.1095$). (Figure 15).

Table 6: (Rearranged slides) Summary data of follicle count per gamma dose exposure.									
Dose (cGy)	Primordial			Primary			Secondary		
	Mean	SD	SEM	Mean	SD	SEM	Mean	SD	SEM
0	671.3	218.8	109.4	223.8	138.9	69.5	181.3	53.8	26.9
5	503.8	240.0	120.0	181.3	98.8	49.4	118.8	44.8	22.4
15	618.8	344.2	172.1	322.5	208.7	104.4	163.8	76.6	38.3
50	1.7	2.9	1.7	0	0	0	75	27.8	16.1
Number of counted ovaries = 15									
SD: Standard Deviation									
SEM: Standard Error of Mean									

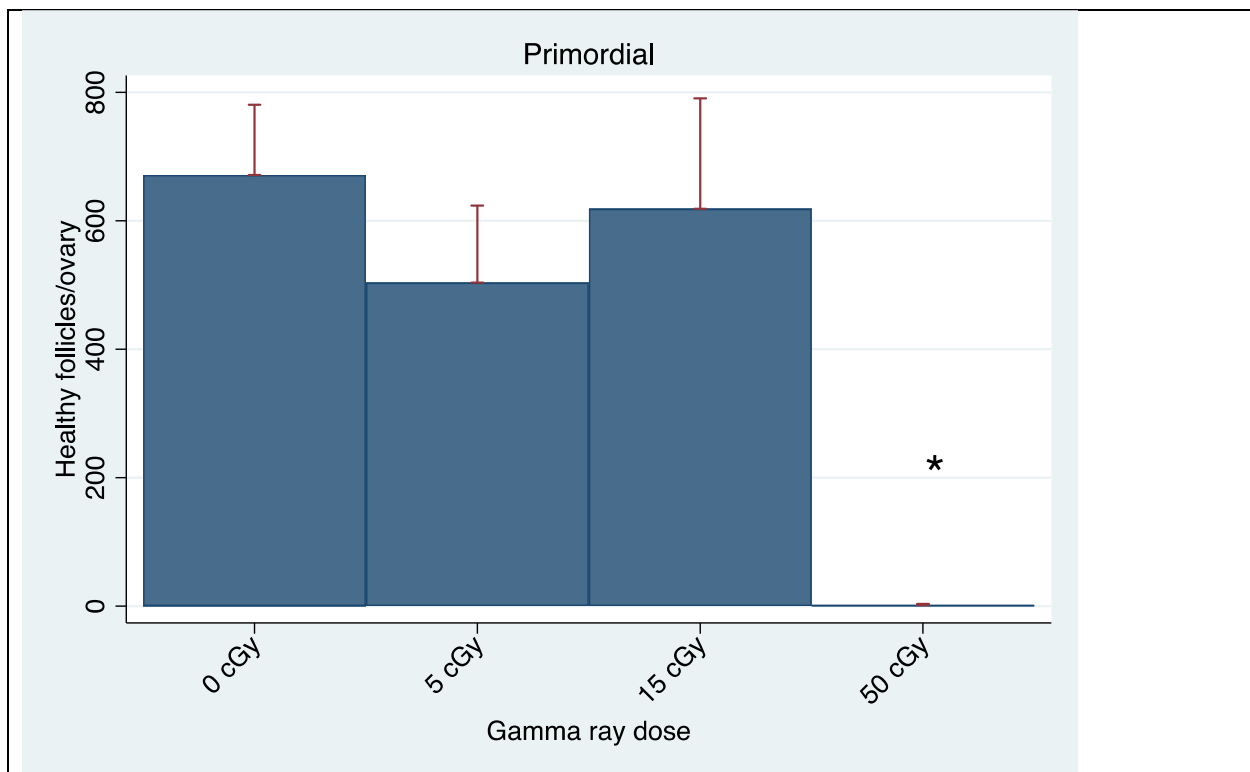


Figure 13. Primordial follicles counts. Gamma irradiation caused depletion of ovarian follicles.

N = 3-4 mice/dose group. Graphs shows the mean \pm S.E.M. of number healthy primordial follicles 1 week after varying doses of gamma irradiation. Graph shows dose dependent depletion of primordial follicles with increasing dose concentration. There is statistically significance difference in the means of the follicle counts among the different dose groups ANOVA; $p = 0.0202$. 15 cGy gamma irradiation caused an increase in number of healthy follicles counted compared to 5 cGy. However, this increased count was not statistically significant after pairwise comparisons of marginal linear predictions and by Mann-Whitney rank-sum test. 50 cGy gamma radiation caused statistically significant (*) complete total destruction of primordial follicles 1-week after irradiation.

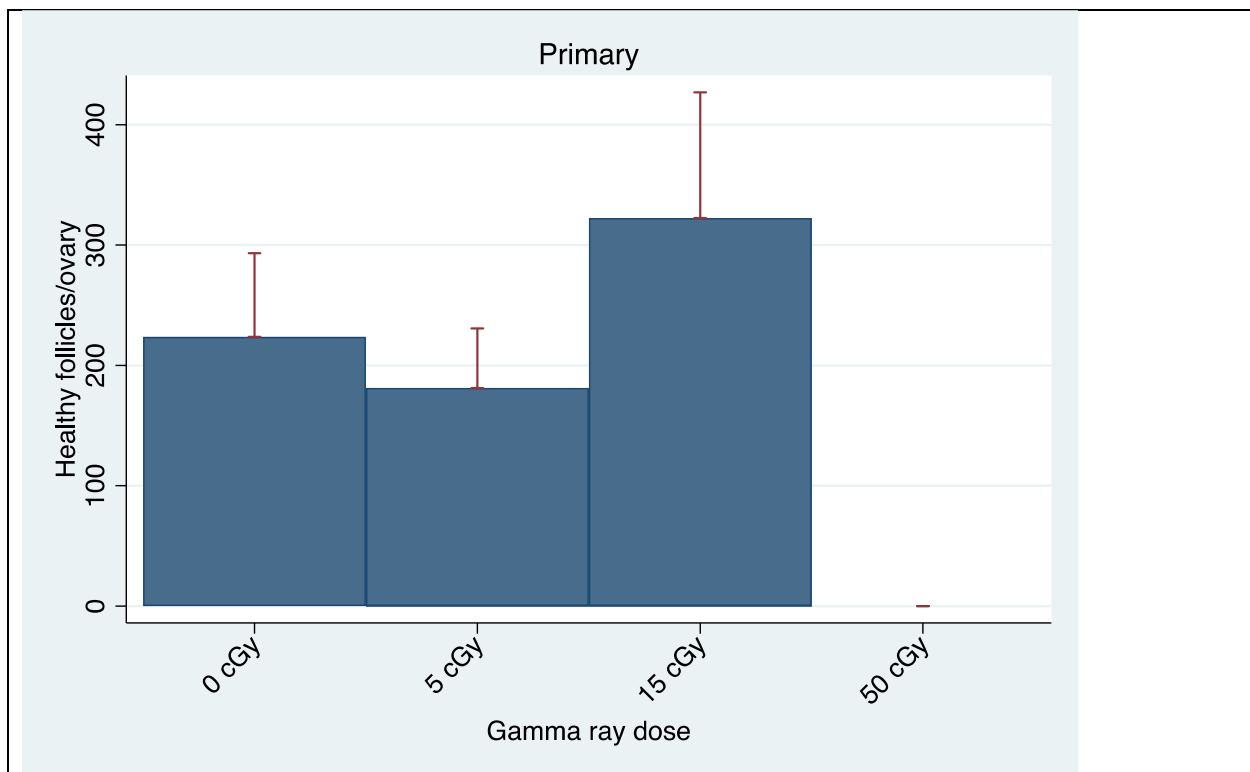


Figure 14. Primary follicles counts. Gamma irradiation caused depletion of primary ovarian follicles. N = 3-4 mice/dose group. Graphs shows the mean \pm S.E.M. of number healthy primary follicles 1 week after varying doses of gamma irradiation. Graph shows a pattern of dose dependent depletion of primary follicles with increasing concentration except for 15 cGy dose. The difference in the means of the follicle counts among the different dose groups didn't show statistically significance ANOVA; $P = 0.0722$. 50 cGy gamma radiation caused complete total destruction of primary follicles 1-week after irradiation.

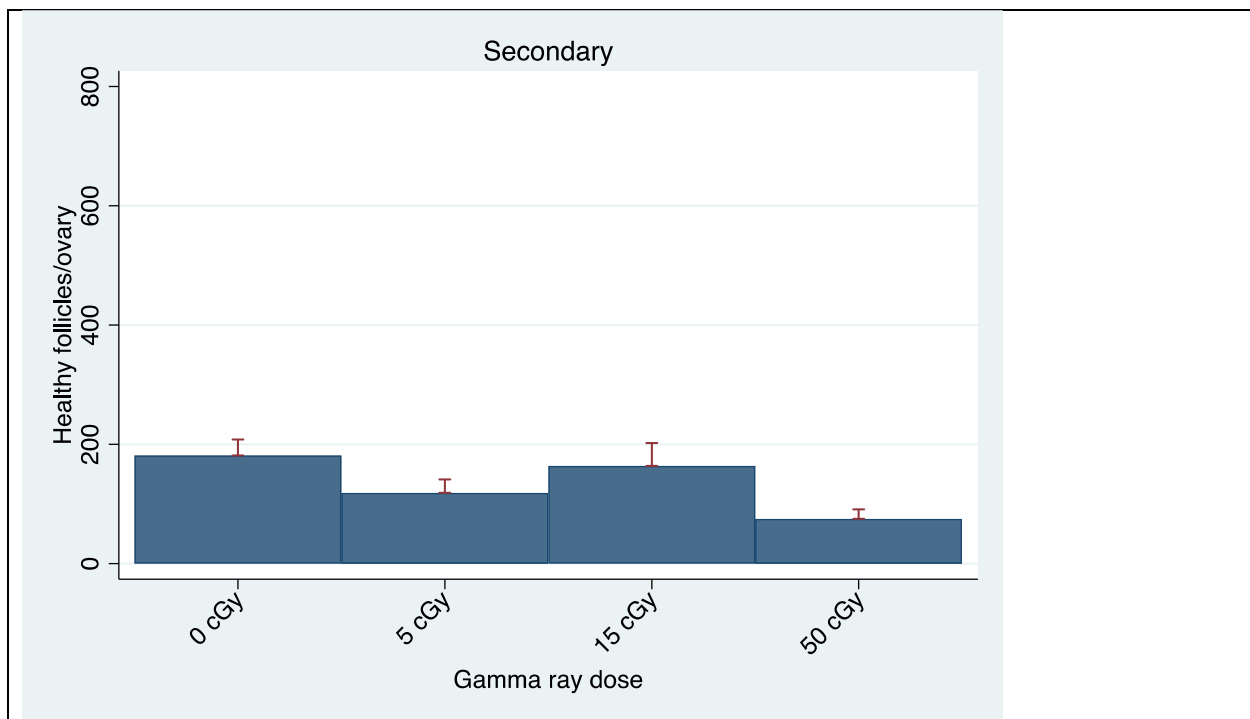


Figure 15. Secondary follicles count. Gamma irradiation caused depletion of secondary ovarian follicles. N = 3-4 mice/dose group. Graphs shows the mean \pm S.E.M. of number healthy secondary follicles 1 week after varying doses of gamma irradiation. Graph shows dose dependent depletion of secondary follicles with increasing dose concentration. There's no statistically significant difference in the means of the follicle counts among the different dose groups ANOVA; $p = 0.1095$.

CHAPTER 5: DISCUSSION

Radioprotection of female reproductive organs and preservation of fertility continues to be critically important especially in patients undergoing cancer treatments and in occupations exposed to higher-than-normal levels of ionizing radiation such as astronauts. The first step to achieving radioprotective goals includes further understanding of the molecular mechanisms and pathways by which ionizing radiation exerts its repro-toxic effects. Therefore, this study investigated the full dose-response effects of varying doses of low LET gamma radiation including 50 cGy on ovarian follicles. Till date, only few published studies have investigated the effects of doses of gamma radiation lower than 50cGy on ovarian follicles. We report a clear dose-dependent reduction in total body weight and ovarian primordial, primary, and secondary follicle numbers in sexually mature female mice after total body irradiation (TBI) with low LET gamma irradiation.

We demonstrated that total body gamma irradiation causes reduction in total body weight. As previously mentioned in both animal and human studies, radiation exposure via either TBI or targeted abdomino-pelvic irradiation is associated with radiation induced connective tissue fibrosis, sclerosis, vascular endothelial cell injury, and spontaneous sclerosis of arteries and arterioles which can lead to pathological reduction in the affected organ morphology and size (Grigsby PW et al., 1995, Straub et al., 2015, Weintraub et al. 2010). These long-term consequences can take years to clinically manifest. Previous studies have reported cranial irradiation in rats resulted in impaired weight gain and stunted growth in a dose dependent pattern. Overmier et al., 1979 exposed three groups of young male albino Wistar rats to X-ray irradiation cranially at 1200, 2400 and 3000 rads and measured growth rate, discrimination learning and sound stimulated exploration. At the end of 15 weeks, they reported significant

clinical impairment in learning and growth rates compared to control non-irradiated rats. Although we also observed overall reduction in the wet uterus and paired ovary+oviduct weights, the effects were not statistically significant. It is possible that 1-week post irradiation was too soon to observe measurable effects of ionizing radiation exposure on the weights of these organs. Another likely explanation is the large estrous cycle stage dependent changes that occur in uterine weights due to uterine ballooning. A way to control for this modifier will require monitoring each mouse estrous cycles and euthanizing the mice on the same estrous cycle stage. However, this approach will lead to lack of uniformity and lack of ability to euthanize all the mice at exactly one week after irradiation. We chose the latter because it was more important for comparison with the ovarian follicle counts from prior studies, and because estrous cycle stage does not affect the numbers of primordial, primary, and secondary follicles, in contrast to antral follicles.

We demonstrated that 50 cGy radiation caused complete destruction of primordial and primary follicles at 1-week post irradiation, while it caused 59% depletion of secondary follicles. This observed follicle stage dependent response to radiation follows a pattern observed in other recent studies. Kimler et al., 2018 exposed sexually mature female mice to 10 cGy and 100 cGy gamma radiation. They reported that early growing (i.e. preantral) follicles stages were significantly depleted after 100 cGy irradiation while larger follicles in later development stages (antral follicles) had equal or greater numbers after irradiation. This finding is consistent with data from previous rodent studies supporting that early follicle stages (i.e., primordial-primary-secondary- in the order of development and size) are more radiosensitive to ionizing radiation while follicles in later stages (i.e., antral and preovulatory) are less radiosensitive (Baker, 1971,

Adriaens et al. 2009, Said et al., 2012, Kimler et al., 2018, Mantawy et al., 2019). Our results support that preantral follicles are highly radiosensitive, especially primordial follicles.

Mishra et al. 2016 reported that high LET charged iron (^{56}Fe) particle radiation (LET = 179 keV/ μm) induced oxidative damage, apoptosis, double stranded DNA breakage and significant follicle depletion of 12-week-old C57BL/6J female mice at 1 week after irradiation at doses of 30 and 50 cGy. In 2017, Mishra et al. reported that high LET charged oxygen (^{16}O) particle radiation caused dose dependent increase in DNA damage, oxidative damage and apoptosis, complete destruction of primordial and primary follicles and elevation of gonadotropin hormones (LH and FSH) in female mice of the same age and strain as in the present study 1-week after irradiation at doses of 30 and 50 cGy. The authors reported an unexpected observation in which the high LET charged oxygen (^{16}O) particle (lower LET = 16.5 keV/ μm - than iron ^{56}Fe) was a more potent destroyer of primordial follicles than higher LET charged ^{56}Fe particles. Thus, suggesting charged ^{16}O particle may have a higher RBE than charged ^{56}Fe particle radiation. This assumption can cautiously be made given that high LET charged oxygen(^{16}O) had a higher energy fluence (number of particles received by a surface per unit area) of about 1.91×10^7 ^{16}O ions/ cm^2 than high LET, charged iron (^{56}Fe) particles (179 keV/ μm), which had a fluence of 1.835×10^6 Fe ions/ cm^2 . This can be interpreted that at the same radiation dose, more oxygen particles than iron particles will traverse a primordial follicle and cause cellular destruction. Despite this difference, both ^{16}O and ^{56}Fe clearly have highly deleterious biological properties. High LET charged particle radiation proportionally generates complex clustered dsDNA damage with LET up to about 300 keV/ μm (Weber & Flentje 1993, Ward J.F. 1994, Prise et al.,1999, and Sutterland et al., 2000). These complex clustered dsDNA breaks are more likely to be poorly repaired due to the challenges they present to cellular repair

mechanism within the follicles compared to lesions created by indirect DNA damage caused by sparsely penetrating low LET gamma radiation. Greater lethality, cytotoxicity, mutagenicity, and genomic instability are observed after high LET exposure. The complexity of DSBs increases with the particle tract core diameter (Weber & Flentje 1993 and Jezkova et al., 2017). Given that gamma rays are photon energy, they carry no charge and have significantly lower LET ranges from 0.66 to 0.8 keV/ μm , one can estimate that fewer ^{137}Cs gamma rays will transverse the ovarian follicle. The distinguishing genotoxic mechanisms between low LET and high-LET radiation are not fully understood and continue to be an ongoing field of research.

Wallace et al. 2003 estimated the ED₅₀ for follicle depletion in female humans to be less than 2 Gy. Data from Mishra 2016 and 2017 studies estimated the ED₅₀ for primordial follicle depletion in female mice at 1-week post high LET charged iron particle radiation was 27.5 cGy and for high LET charged oxygen particle radiation was 4.6 cGy. Our current preliminary data is not sufficient to allow accurate estimation of the ED₅₀ for gamma radiation, but based on our data thus far, we cautiously conclude that it is between 15 cGy and 50 cGy.

The mechanism by which gamma radiation induces ovarian destruction and depletion of the ovarian reserve is still not completely understood. However, a number of in vitro and in vivo studies have investigated and proposed molecular pathways involved in gamma radiation induced oocyte apoptosis. A number of molecular mechanisms are involved in gamma radiation-induced ovo- toxicity. In summary they include a) oxidative stress and generation of toxic free radicals and reactive oxygen species (ROS); b) activation of inflammatory cascade within the ovary and surrounding cells; c) DNA damage and mitochondrial dysfunction leading to activation of the intrinsic apoptotic pathway; d) disruption of hormonal regulation of folliculogenesis. Low LET gamma irradiation causes single and double stranded DNA breaks but

generation of ROS from radiolysis of water is reported to account for the majority of DNA damage (Cadet et al., 1999, Spitz et al., 2004; Dayal et al., 2008). These ROS induce oxidative stress and damage essential cellular molecules and structures such as DNA, lipids, proteins and alter membrane integrity (Cadet et al., 2004, Cadet et al., 2005). Misrepair of DNA damage can lead to cell death by apoptosis. Cortés-Wanstreet et al., 2009 revealed that generated ROS rapidly increased in human COV434 granulosa cells within 30 mins after 1 or 5 Gy gamma irradiation, and ROS remained persistently elevated for at least 48 h; induction of apoptosis was evident at 6h. Notably in the same study, overexpression of glutamate cysteine ligase subunits to enhance glutathione synthesis prevented radiation induced elevation in ROS and apoptotic death. Acute gamma irradiation caused measurable increase in ovarian and uterine lipid peroxides, depletion of GSH and decreased enzymatic activity of antioxidants in irradiated rats (Said et al., 2012). IR-induced ROS generation can activate cellular apoptosis (Shinomiya 2001 and Feinendegan 2002).

Post irradiation inflammatory changes lead to activation of pro-inflammatory cytokines and chemokines which can further promulgated chronic inflammation and tissue injury (Martin et al., 2000). One key cellular inflammatory cytokine is the tissue necrosis factor alpha (TNF- α). Mantawy et al., 2019 extensively investigated the mechanism for IR induced premature ovarian failure by exposing rats to 3.2 Gy gamma radiation. The authors measured significantly higher levels of inflammatory markers in irradiated rats compared to non-irradiated rats. They reported 28% higher ovarian TNF- α (measured by ELISA); increased NF-kB p65 (an inflammatory marker) immunoreactivity in the cytoplasm of follicular oocyte, granulosa cells, theca cells, and ovarian stromal cells via immunohistochemical staining; elevation of proinflammatory enzymes iNOS and COX-2 immunoreactivity mainly in the granulosa and theca cells of the ovary.

Ovarian TGF- β cytokine levels was elevated by 225% in irradiated ovaries, and both phosphorylated forms of p38 and JNK was elevated. Thus, the activation of TGF- β / MAPK signaling pathways is implicated in gamma radiation induced ovarian follicular injury. Electron microscopic examination of gamma irradiated ovarian tissues showed abnormal mitochondrial ultrastructural aberrations such as swelling, cristae disorder and vacuolation. Wang et al., 2019 reported that mitochondrial distribution and mass were not affected by gamma radiation in primordial follicles however they measured transient loss in mitochondrial membrane potential in 20-40% of primary and primordial follicles at 3-6 hours after 10 cGy irradiation. This indicated that the mitochondria were compromised and could have contributed to induction of apoptosis. However, the authors could not distinguish if oocytes undergoing apoptosis was secondary to the direct damage of the mitochondrial by gamma radiation or result of damage to nuclear DNA (Wang et al., 2019).

One of the well published molecular pathway mechanisms is the mitochondrial pathway of apoptosis in primordial follicles. Gamma irradiation direct and indirect damage causes genotoxic stress and leads to DNA DSBs within the oocyte (Hanoux et al. 2006; Suh et al. 2006). Detection of the presence of DSBs within the nucleus leads to the phosphorylation of p63. Phosphorylated p63 activates the transcription of pro-apoptotic enzymes and commits the oocyte to apoptotic pathway (Livera et al., 2008). Livera et al. 2008 demonstrated that p63 is produced and TAP63 alpha is activated by phosphorylation in response to the presence of DNA DSBs which consequently induces apoptosis in primordial follicles. TAP63 α is the main isoform of p63 involved in radiation-induced apoptosis in oocytes (Suh et al., 2006). p63 transcription factor is part of the p53 family of transcription factors. Suh et al., 2006 reported the presence of TAP63 expression in oocyte nucleus in all preantral follicles and absence in antral follicles. Gonfloni et

al., 2009 identified that TAp63 is phosphorylated by c-Abl tyrosine kinase in chemotherapy (cisplatin) treated mice. Kerr et al., 2012 demonstrated TAp63 activation mediates the transcriptional induction of BH3-only proapoptotic B-cell lymphoma-2 (BCL-2) family members namely PUMA and NOXA in primordial follicles. BCL-2 family protein are regulators of programmed cell death (Youle & Strasser). Kerr et al., 2012 also revealed that primordial, primary and secondary follicles in mice with PUMA knock-out mutation and combined knock-out of PUMA and NOXA mutations were significantly rescued from gamma irradiation DNA damaged induced apoptosis thus preserving the ovarian reserve. PUMA and NOXA in turn mediate apoptosis by activating proapoptotic BCL-2 family member effector molecules BAX and BAK while binding and inhibiting pro-survival BCL-2 members (Chipuk & Green, 2008; Youle & Strasser, 2008). Conformational changes of BAX and BAK proteins leads to permeability of the outer membrane of the mitochondria, release of cytochrome c and consequent activation of caspase proteases leading to cell death (Youle & Strasser, 2008). ROS induced mitochondrial membrane damage also leads to release of cytochrome c into the cytosol which activates caspases thus triggering apoptosis (England & Cotter 2005). Hanoux et al., 2007 observed increased caspase -2 immunostaining in both the cytoplasm and nucleus and downstream activation of caspase -9 and -3 in gamma irradiated oocytes. Caspase -2,-9 and -3 are proapoptotic enzymes and their levels are good indicator of apoptosis. Treatment with a caspase-2 inhibitor prevented the downstream activation of caspase 9 and 3 in some oocytes, however, the majority of the oocytes were nonetheless destroyed. Thus, the authors concluded that the caspase-2 activated mitochondrial pathway is not the sole mechanism involved in the trigger of oocyte apoptosis after radiation-induced genotoxic stress. In another study, gamma

irradiation caused significant elevation in caspase 3 and cytochrome c expression in ovarian granulosa and theca cells and in uterine tissues (Said et al., 2012).

Another mechanism worth mentioning is post radiation endocrine dysfunction and estradiol deficiency. As discussed earlier, estradiol plays a major role in follicle development and prevents granulosa cell apoptosis (CRC Press 2015). Estradiol is a predictive factor for assessing ovarian reserve. Premature ovarian failure is characterized by hypergonadotropic hypogonadism i.e estradiol deficiency and consequent elevation in FSH (Ataya et al., 1985 and Miyazaki et al., 2015). In the current study, although no hormonal measurement was analyzed, we observed complete destruction of primordial and primary follicles and near depletion of secondary follicles 1-week post gamma irradiation. Although I did not count antral follicles, prior studies have reported remarkable reductions in estradiol and multi-fold increase in FSH levels after gamma irradiation (Said et al., 2012 and Mantawy et al., 2019). Post radiation estradiol deficiency and elevated FSH concentration may predispose cells to apoptosis resulting in radiation-induced ovarian follicle destruction and depletion of follicular reserve.

CHAPTER 6: CONCLUSION

The difference between follicle loss seen in normal physiologic reproductive aging compared to radiation induced is that radiation exposure causes accelerated follicle loss consequently leading to early senescence. In our mouse model of low LET gamma radiation-induced damage, we observed complete primordial and primary follicle loss, greater than 50% secondary follicle loss and reduction in total body weight in the absence of statistically significant reduction in wet uterus and ovary+oviduct weights. We acknowledge that due to our TBI model, we cannot directly distinguish if the observed follicle loss and total body weight reduction is due to direct insult to the female reproductive system or instead due to indirect systemic effects. However, similarly reported findings from in vitro studies in which ovaries were irradiated support that our findings are the result of direct radiation insult.

We believe that our observations can provide a valuable insight into the chronological mechanisms that drive normal physiological reproductive aging. Current and future studies using TBI mouse model will help investigate the differences between acute, subacute and chronic effects of ionizing radiation induced female ovotoxicity and help to determine whether the mechanisms seen in occupation radiation exposure and normal reproductive aging are distinct or similar to each other.

REFERENCE

- Adriaens, I., Smitz, J. and Jacquet, P., 2009. The current knowledge on radiosensitivity of ovarian follicle development stages. *Human reproduction update*, 15(3), pp.359-377.
- Agency for Toxic Substances and Disease Registry (ATSDR). 1999. Toxicological profile for ionizing radiation. Atlanta, GA: U.S. Department of Health and Human Services, Public Health Service.
- Agha, A., Sherlock, M., Brennan, S., O'Connor, S.A., O'Sullivan, E., Rogers, B., Faul, C., Rawluk, D., Tormey, W. and Thompson, C.J., 2005. Hypothalamic-pituitary dysfunction after irradiation of nonpituitary brain tumors in adults. *The Journal of Clinical Endocrinology & Metabolism*, 90(12), pp.6355-6360.
- Ataya, K.M., McKanna, J.A., Weintraub, A.M., Clark, M.R. and LeMaire, W.J., 1985. A luteinizing hormone-releasing hormone agonist for the prevention of chemotherapy-induced ovarian follicular loss in rats. *Cancer research*, 45(8), pp.3651-3656.
- Autsavapromporn, N., De Toledo, S.M., Little, J.B., Jay-Gerin, J.P., Harris, A.L. and Azzam, E.I., 2011. The role of gap junction communication and oxidative stress in the propagation of toxic effects among high-dose α -particle-irradiated human cells. *Radiation research*, 175(3), pp.347-357.
- Baerwald, Angela R., Gregg P. Adams, and Roger A. Pierson. "Ovarian antral folliculogenesis during the human menstrual cycle: a review." *Human reproduction update* 18.1 (2012): 73-91.
- Baker TG. Comparative aspects of the effects of radiation during oogenesis, *Mutat Res*, 1971, vol. 11 (pg. 9-22)

- Bath, L.E., Critchley, H.O., Chambers, S.E., Anderson, R.A., Kelnar, C.J. and Wallace, W.H.B., 1999. Ovarian and uterine characteristics after total body irradiation in childhood and adolescence: response to sex steroid replacement. *BJOG: An International Journal of Obstetrics & Gynaecology*, 106(12), pp.1265-1272.
- Bekker-Jensen, Simon, and Niels Mailand. "Assembly and Function of DNA Double-Strand Break Repair Foci in Mammalian Cells." *DNA Repair* 9.12 (2010): 1219–1228. Web.
- Cadet, J., Delatour, T., Douki, T., Gasparutto, D., Pouget, J.P., Ravanat, J.L. and Sauvaigo, S., 1999. Hydroxyl radicals and DNA base damage. *Mutation Research/Fundamental and Molecular Mechanisms of Mutagenesis*, 424(1-2), pp.9-21.
- Cadet, J., Douki, T., Gasparutto, D. and Ravanat, J.L., 2005. Radiation-induced damage to cellular DNA: measurement and biological role. *Radiation Physics and Chemistry*, 72(2-3), pp.293-299.
- Cadet, J., Bellon, S., Douki, T., Frelon, S., Gasparutto, D., Muller, E., Pouget, J.P., Ravanat, J.L., Romieu, A. and Sauvaigo, S., 2004. Radiation-induced DNA damage: formation, measurement, and biochemical features. *Journal of Environmental Pathology, Toxicology and Oncology*, 23(1).
- Canning, J., Takai, Y. and Tilly, J.L., 2003. Evidence for genetic modifiers of ovarian follicular endowment and development from studies of five inbred mouse strains. *Endocrinology*, 144(1), pp.9-12.
- Chieng PU, Huang TS, Chang CC, Chong PN, Tien RD, Su CT. Reduced hypothalamic blood flow after radiation treatment of nasopharyngeal cancer: SPECT studies in 34 patients. *Am J Neuroradiol*. 1991;12:661–5.

- Chipuk, J.E. and Green, D.R., 2008. How do BCL-2 proteins induce mitochondrial outer membrane permeabilization?. *Trends in cell biology*, 18(4), pp.157-164.
- Choudhury, Ananya, Andrew Cuddihy, and Robert G Bristow. "Radiation and New Molecular Agents Part I: Targeting ATM-ATR Checkpoints, DNA Repair, and the Proteasome." *Seminars in Radiation Oncology* 16.1 (2006): 51–58. Web.
- Collins, Josie K ; Jones, Keith T. "DNA Damage Responses in Mammalian Oocytes." *Reproduction* 152.1 (2016): R15–R22. Web.
- Computational Methods for Reproductive and Developmental Toxicology. United Kingdom, CRC Press, 2015.
- Constine, L.S., Woolf, P.D., Cann, D., Mick, G., McCormick, K., Raubertas, R.F. and Rubin, P., 1993. Hypothalamic-pituitary dysfunction after radiation for brain tumors. *New England Journal of Medicine*, 328(2), pp.87-94.
- Cortes-Wanstreet, M.M., Giedzinski, E., Limoli, C.L. and Luderer, U., 2009. Overexpression of glutamate–cysteine ligase protects human COV434 granulosa tumour cells against oxidative and γ -radiation-induced cell death. *Mutagenesis*, 24(3), pp.211-224.
- Critchley, H.O.D., Wallace, W.H.B., Shalet, S.M., Mamtora, H., Higginson, J. and Anderson, D.C., 1992. Abdominal irradiation in childhood; the potential for pregnancy. *BJOG: An International Journal of Obstetrics & Gynaecology*, 99(5), pp.392-394.
- Critchley, Hilary OD, and W. Hamish B. Wallace. "Impact of cancer treatment on uterine function." *JNCI Monographs* 2005.34 (2005): 64-68.
- Cucinotta, Francis A., and Marco Durante. "Risk of radiation carcinogenesis." *Human health and performance risks of space exploration missions*. NASA SP-2009-3405. Houston: National Aeronautics and Space Administration (2009): 119-170.

- Dayal, D., Martin, S.M., Limoli, C.L. and Spitz, D.R., 2008. Hydrogen peroxide mediates the radiation-induced mutator phenotype in mammalian cells. *Biochemical Journal*, 413(1), pp.185-191.
- de Ziegler, D., Fraisse, T., de Candolle, G., Vulliemoz, N., Bellavia, M. and Colamaria, S., 2007. Roles of FSH and LH during the follicular phase: insight into natural cycle IVF. *Reproductive biomedicine online*, 15(5), pp.507-513.
- Dietze, G., Bartlett, D. T., Cool, D. A., Cucinotta, F. A., Jia, X., McAulay, I. R., ... & Sato, T. (2013). Icrp publication 123: Assessment of radiation exposure of astronauts in space. *Annals of the ICRP*, 42(4), 1-339.
- Durante, M. and Cucinotta, F.A., 2008. Heavy ion carcinogenesis and human space exploration. *Nature Reviews Cancer*, 8(6), pp.465-472.
- Eisenbud, M., 1984. Sources of ionizing radiation exposure. *Environment: Science and Policy for Sustainable Development*, 26(10), pp.6-33.
- Elisabeth C. Larsen, Kjeld Schmiegelow, Catherine Rechnitzer, Anne Loft, Jørn Müller & Anders Nyboe Andersen (2004) Radiotherapy at a young age reduces uterine volume of childhood cancer survivors, *Acta Obstetrica et Gynecologica Scandinavica*, 83:1, 96-102
- England, K., and T. G. Cotter. "Direct oxidative modifications of signalling proteins in mammalian cells and their effects on apoptosis." *Redox Report* 10.5 (2005): 237-245.
- Fauci, Anthony S. *Harrison's Principles of Internal Medicine*. 20th ed. New York, N.Y: McGraw-Hill Education LLC, 2018. Web.
- Gonfloni, S., Di Tella, L., Caldarola, S., Cannata, S.M., Klinger, F.G., Di Bartolomeo, C., Mattei, M., Candi, E., De Felici, M., Melino, G. and Cesareni, G., 2009. Inhibition of the

- c-Abl–TAp63 pathway protects mouse oocytes from chemotherapy-induced death. *Nature medicine*, 15(10), pp.1179-1185.
- Goodhead, D.T., 1994. Initial events in the cellular effects of ionizing radiations: clustered damage in DNA. *International journal of radiation biology*, 65(1), pp.7-17.
- Feinendegen, L. E. "Reactive oxygen species in cell responses to toxic agents." *Human & experimental toxicology* 21.2 (2002): 85-90.
- Fiorenza, M.T., Bevilacqua, A., Bevilacqua, S. and Mangia, F., 2001. Growing dictyate oocytes, but not early preimplantation embryos, of the mouse display high levels of DNA homologous recombination by single-strand annealing and lack DNA nonhomologous end joining. *Developmental biology*, 233(1), pp.214-224.
- Findlay, Jock K. "Folliculogenesis." (2003): 653-656.
- Gibson, K., 2014. *Women in Space: 23 Stories of First Flights, Scientific Missions, and Gravity-Breaking Adventures*. Chicago Review Press.
- Gosden, R.G., Laing, S.C., Felicio, L.S., Nelson, J.F. and Finch, C.E., 1983. Imminent oocyte exhaustion and reduced follicular recruitment mark the transition to acyclicity in aging C57BL/6J mice. *Biology of reproduction*, 28(2), pp.255-260.
- Grigsby, P.W., Russell, A., Bruner, D., Eifel, P., Koh, W.J., Spanos, W., Stetz, J., Stitt, J.A. and Sullivan, J., 1995. Late injury of cancer therapy on the female reproductive tract. *International Journal of Radiation Oncology* Biology* Physics*, 31(5), pp.1281-1299.
- Halperin EC, Wazer DE, Perez CA, Brady LW. *Perez & Brady's Principles and Practice of Radiation Oncology*. 7th ed. Philadelphia, PA: Wolters Kluwer; 2018.

- Hanoux, V., Pairault, C., Bakalska, M., Habert, R. and Livera, G., 2007. Caspase-2 involvement during ionizing radiation-induced oocyte death in the mouse ovary. *Cell Death & Differentiation*, 14(4), pp.671-681.
- Heijink, A.M., M. Krajewska, and M.A.T.M. van Vugt. "The DNA Damage Response During Mitosis." *Mutation Research - Fundamental and Molecular Mechanisms of Mutagenesis* 750.1-2 (2013): 45–55. Web
- Hennebold, J. D. in *Encyclopedia of Reproduction: Volume 2 Female Reproduction* 2nd edn (eds T. E. Spencer & J. A. Flaws) 99–105 (Elsevier, 2018).
- Hirshfield AN. Size-frequency analysis of Atresia in cycling rats. *Biol Reprod* 1988;38:1181–1188.
- Hirshfield AN. Overview of ovarian follicular development: considerations for the toxicologist. *Environ Mol Mutagen* 1997;29:10–15.
- Hochberg Z, Kuten A, Hertz P, Thatcher M, Kedar A, Benderly A. The effect of single-dose radiation on cell survival and growth hormone secretion by rat anterior pituitary cells. *Radiat Res.* 1983;94:508–12.
- Holm, K., Nysom, K., Brocks, V., Hertz, H., Jacobsen, N. and Müller, J., 1999. Ultrasound B-mode changes in the uterus and ovaries and Doppler changes in the uterus after total body irradiation and allogeneic bone marrow transplantation in childhood. *Bone marrow transplantation*, 23(3), pp.259-263.
- ICRP 2003 Relative biological effectiveness (RBE), quality factor (Q), and radiation weighting factor (w_R). ICRP Publication 92. *Annals of the ICRP* 33 1–121. (doi:10.1016/s0146-6453(03)00024-1)

- Jennings, Richard T., and Ellen S. Baker. "Gynecological and reproductive issues for women in space: a review." *Obstetrical & gynecological survey* 55.2 (2000): 109.
- Jezkova, L., Zadneprianetc, M., Kulikova, E., Smirnova, E., Bulanova, T., Depes, D., Falkova, I., Boreyko, A., Krasavin, E., Davidkova, M. and Kozubek, S., 2018. Particles with similar LET values generate DNA breaks of different complexity and reparability: a high-resolution microscopy analysis of γ H2AX/53BP1 foci. *Nanoscale*, 10(3), pp.1162-1179.
- Jungmichel, S. and Stucki, M., 2010. MDC1: The art of keeping things in focus. *Chromosoma*, 119(4), pp.337-349.
- Kerr, J.B., Hutt, K.J., Michalak, E.M., Cook, M., Vandenberg, C.J., Liew, S.H., Bouillet, P., Mills, A., Scott, C.L., Findlay, J.K. and Strasser, A., 2012. DNA damage-induced primordial follicle oocyte apoptosis and loss of fertility require TAp63-mediated induction of Puma and Noxa. *Molecular cell*, 48(3), pp.343-352.
- Keith, S., Murray, H.E. and Spoo, W., 1999. Toxicological profile for ionizing radiation.
- Khanna, K.K., Lavin, M.F., Jackson, S.P. and Mulhern, T.D., 2001. ATM, a central controller of cellular responses to DNA damage. *Cell Death & Differentiation*, 8(11), pp.1052-1065.
- Kim JK, Lee CJ. Effect of exogenous melatonin on the ovarian follicles in Y-irradiated mouse. *Mutat Res* 2000;449:33–39.
- Kimler, B.F., Briley, S.M., Johnson, B.W., Armstrong, A.G., Jasti, S. and Duncan, F.E., 2018. Radiation-induced ovarian follicle loss occurs without overt stromal changes. *Reproduction*, 155(6), pp.553-562.
- Klaassen, C.D. and Amdur, M.O. eds., 2013. Casarett and Doull's toxicology: the basic science of poisons (Vol. 1236, p. 189). New York: McGraw-Hill.

- Kristoffer Valerie, and Lawrence F Povirk. "Regulation and Mechanisms of Mammalian Double-Strand Break Repair." *Oncogene* 22.37 (2003): 5792–5812. Web.
- Kujjo, L.L., Laine, T., Pereira, R.J., Kagawa, W., Kurumizaka, H., Yokoyama, S. and Perez, G.I., 2010. Enhancing survival of mouse oocytes following chemotherapy or aging by targeting Bax and Rad51. *PloS one*, 5(2), p.e9204.
- Kuo, L.J. and Yang, L.X., 2008. γ -H2AX-a novel biomarker for DNA double-strand breaks. *In vivo*, 22(3), pp.305-309.
- Kutluk, O., Volkan, T., Shiny, T., Robert, S. and Lin, L., 2015. BRCA mutations. DNA repair deficiency, and ovarian aging. *Biol. Reprod*, 93, p.67.
- Hall, E.J. and Giaccia, A.J., 2006. *Radiobiology for the Radiologist* (Vol. 6).
- Larsen, E.C., Schmiegelow, K., Rechnitzer, C., Loft, A., Müller, J. and Andersen, A.N., 2004. Radiotherapy at a young age reduces uterine volume of childhood cancer survivors. *Acta obstetricia et gynecologica Scandinavica*, 83(1), pp.96-102.
- Lee, C.J., Park, H.H., Do, B.R., Yoon, Y.D. and Kim, J.K., 2000. Natural and radiation-induced degeneration of primordial and primary follicles in mouse ovary. *Animal Reproduction Science*, 59(1-2), pp.109-117.
- Lee, C.J. and Yoon, Y.D., 2005. γ -Radiation-induced follicular degeneration in the prepubertal mouse ovary. *Mutation Research/Fundamental and Molecular Mechanisms of Mutagenesis*, 578(1-2), pp.247-255.
- Lieber, Michael R. "The Mechanism of Double-Strand DNA Break Repair by the Nonhomologous DNA End-Joining Pathway." *Annual Review of Biochemistry* 79.1 (2010): 181–211. Web

- Livera, G., Petre-Lazar, B., Guerquin, M.J., Trautmann, E., Coffigny, H. and Habert, R., 2008. p63 null mutation protects mouse oocytes from radio-induced apoptosis. *Reproduction*, 135(1), p.3.
- Lim, J., Lawson, G.W., Nakamura, B.N., Ortiz, L., Hur, J.A., Kavanagh, T.J. and Luderer, U., 2013. Glutathione-deficient mice have increased sensitivity to transplacental benzo [a] pyrene-induced premature ovarian failure and ovarian tumorigenesis. *Cancer research*, 73(2), pp.908-917.
- Little MD, Shalet SM, Beardwell CG, Robinson EL, Sutton ML. Radiationinduced hypopituitarism is dose-dependent. *Clin Endocrinol*. 1989;31: 363–73.
- Lopez, S.G. and Luderer, U., 2004. Effects of cyclophosphamide and buthionine sulfoximine on ovarian glutathione and apoptosis. *Free Radical Biology and Medicine*, 36(11), pp.1366-1377.
- Presti, A.L., Ruvolo, G., Gancitano, R.A. and Cittadini, E., 2004. Ovarian function following radiation and chemotherapy for cancer. *European Journal of Obstetrics & Gynecology and Reproductive Biology*, 113, pp.S33-S40.
- Maidarti, M., Anderson, R.A. and Telfer, E.E., 2020. Crosstalk between PTEN/PI3K/Akt Signalling and DNA Damage in the Oocyte: Implications for Primordial Follicle Activation, Oocyte Quality and Ageing. *Cells*, 9(1), p.200.
- Mantawy, Eman M., Riham S. Said, and Amal Kamal Abdel-Aziz. "Mechanistic approach of the inhibitory effect of chrysin on inflammatory and apoptotic events implicated in radiation-induced premature ovarian failure: Emphasis on TGF- β /MAPKs signaling pathway." *Biomedicine & Pharmacotherapy* 109 (2019): 293-303.

- Marci, R., Mallozzi, M., Di Benedetto, L., Schimberni, M., Mossa, S., Soave, I., Palomba, S. and Caserta, D., 2018. Radiations and female fertility. *Reproductive Biology and Endocrinology*, 16(1), pp.1-12.
- Martin, J.H., Bromfield, E.G., Aitken, R.J., Lord, T. and Nixon, B., 2018. Double strand break DNA repair occurs via non-homologous end-joining in mouse MII oocytes. *Scientific reports*, 8(1), pp.1-15.
- Martin, Michèle, Jean-Louis Lefaix, and Sylvie Delanian. "TGF- β 1 and radiation fibrosis: a master switch and a specific therapeutic target?." *International Journal of Radiation Oncology* Biology* Physics* 47.2 (2000): 277-290.
- Mathur, S., Nandchahal, K. and Bhartiya, H.C., 1991. Radioprotection by MPG of mice ovaries exposed to sublethal gamma radiation doses at different postnatal ages. *Acta Oncologica*, 30(8), pp.981-983.
- Meirow D, Nugent D. The effects of radiotherapy and chemotherapy on female reproduction. *Hum Reprod Update* 2001;7:535–543.
- Miyazaki, K., Miki, F., Uchida, S., Masuda, H., Uchida, H. and Maruyama, T., 2015. Serum estradiol level during withdrawal bleeding as a predictive factor for intermittent ovarian function in women with primary ovarian insufficiency. *Endocrine Journal*, 62(1), pp.93-99.
- Muñoz, M., Santaballa, A., Segui, M.A., Beato, C., de la Cruz, S., Espinosa, J., Fonseca, P.J., Perez, J., Quintanar, T. and Blasco, A., 2016. SEOM Clinical Guideline of fertility preservation and reproduction in cancer patients (2016). *Clinical and Translational Oncology*, 18(12), pp.1229-1236.

- Oktaý, K., Turan, V., Titus, S., Stobezki, R. and Liu, L., 2015. BRCA mutations, DNA repair deficiency, and ovarian aging. *Biology of Reproduction*, 93(3), pp.67-1.
- Overmier JB, Carroll ME, Patten R, Krivit W & Kim TH 1979 Cranial irradiation of young rats impairs later learning and growth. *Physiology and Behavior* 23 179–184.
- Pastina, B. and LaVerne, J.A., 1999. Hydrogen peroxide production in the radiolysis of water with heavy ions. *The Journal of Physical Chemistry A*, 103(11), pp.1592-1597.
- Pesty, A., Doussau, M., Lahaye, J.B. and Lefèvre, B., 2010. Whole-body or isolated ovary ⁶⁰Co irradiation: effects on in vivo and in vitro folliculogenesis and oocyte maturation. *Reproductive Toxicology*, 29(1), pp.93-98.
- Preston, D.L., Shimizu, Y., Pierce, D.A., Suyama, A. and Mabuchi, K., 2003. Studies of mortality of atomic bomb survivors. Report 13: Solid cancer and noncancer disease mortality: 1950–1997. *Radiation research*, 160(4), pp.381-407.
- Pfaffl, Michael W., Graham W. Horgan, and Leo Dempfle. "Relative expression software tool (REST©) for group-wise comparison and statistical analysis of relative expression results in real-time PCR." *Nucleic acids research* 30.9 (2002): e36-e36.
- Pouget, J.P., Frelon, S., Ravanat, J.L., Testard, I., Odin, F. and Cadet, J., 2002. Formation of modified DNA bases in cells exposed either to gamma radiation or to high-LET particles. *Radiation research*, 157(5), pp.589-595.
- Rask, J., Vercoutere, W., Navarro, B. J., & Krause, A. (2008). Space Faring: The Radiation Challenge. *Nasa, Module*, 3(8), 9.
- Ray, K., 2017. Toxicity of Radiation: Biological Effects of Ionizing Radiation Exposure on Reproduction. In *Reproductive and Developmental Toxicology* (pp. 359-375). Academic Press.

- Robinson IC, Fairhall KM, Hendry JH, Shalet SM. Differential radiosensitivity of hypothalamopituitary function in the young adult rat. *J Endocrinol.* 2001;169:519–26.
- Robinson IC, Fairhall KM, Hendry JH, Shalet SM. Differential radiosensitivity of hypothalamopituitary function in the young adult rat.
- Rodgers, Kasey, and Mitch Mcvey. "Error-Prone Repair of DNA Double-Strand Breaks." *Journal of Cellular Physiology* 231.1 (2016): 15–24. Web.
- Said, Riham S., Ahmed S. Nada, and Ebtehal El-Demerdash. "Sodium selenite improves folliculogenesis in radiation-induced ovarian failure: a mechanistic approach." *PLoS One* 7.12 (2012): e50928.
- Samaan, N.A., Vieto, R., Schultz, P.N., Maor, M., Meoz, R.T., Sampiere, V.A., Cangir, A., Ried, H.L. and Jesse Jr, R.H., 1982. Hypothalamic, pituitary and thyroid dysfunction after radiotherapy to the head and neck. *International Journal of Radiation Oncology* Biology* Physics*, 8(11), pp.1857-1867.
- Schulte-Uentrop, L., El-Awady, R.A., Schliecker, L., Willers, H. and Dahm-Daphi, J., 2008. Distinct roles of XRCC4 and Ku80 in non-homologous end-joining of endonuclease-and ionizing radiation-induced DNA double-strand breaks. *Nucleic acids research*, 36(8), pp.2561-2569.
- Shahbazi-Gahrouei, D., Gholami, M. and Setayandeh, S., 2013. A review on natural background radiation. *Advanced biomedical research*, 2.
- Shinomiya, N. "New concepts in radiation-induced apoptosis: 'premitotic apoptosis' and 'postmitotic apoptosis'." *Journal of cellular and molecular medicine* 5.3 (2001): 240-253.
- So, S., Davis, A.J. and Chen, D.J., 2009. Autophosphorylation at serine 1981 stabilizes ATM at DNA damage sites. *Journal of Cell Biology*, 187(7), pp.977-990.

- Spitz, D.R., Azzam, E.I., Li, J.J. and Gius, D., 2004. Metabolic oxidation/reduction reactions and cellular responses to ionizing radiation: a unifying concept in stress response biology. *Cancer and Metastasis Reviews*, 23(3-4), pp.311-322.
- Sridharan, D.M., Asaithamby, A., Bailey, S.M., Costes, S.V., Doetsch, P.W., Dynan, W.S., Kronenberg, A., Rithidech, K.N., Saha, J., Snijders, A.M. and Werner, E., 2015. Understanding cancer development processes after HZE-particle exposure: roles of ROS, DNA damage repair and inflammation. *Radiation research*, 183(1), pp.1-26.
- Straub JM, New J, Hamilton CD, Lominska C, Shnayder Y & Thomas SM 2015 Radiation-induced fibrosis: mechanisms and implications for therapy. *Journal of Cancer Research and Clinical Oncology* 141 1985–1994.
- Stringer, J.M., Winship, A., Liew, S.H. and Hutt, K., 2018. The capacity of oocytes for DNA repair. *Cellular and molecular life sciences*, 75(15), pp.2777-2792.
- Suh, E.K., Yang, A., Kettenbach, A., Bamberger, C., Michaelis, A.H., Zhu, Z., Elvin, J.A., Bronson, R.T., Crum, C.P. and McKeon, F., 2006. p63 protects the female germ line during meiotic arrest. *Nature*, 444(7119), pp.624-628.
- Suntharalingam, N.A.G.A.L.I.N.G.A.M., Podgorsak, E.B. and Hendry, J.H., 2005. Basic radiobiology. *Radiation oncology physics: A handbook for teachers and students*, pp.485-504.
- Sutherland, B.M., Bennett, P.V., Sidorkina, O. and Laval, J., 2000. Clustered DNA damages induced in isolated DNA and in human cells by low doses of ionizing radiation. *Proceedings of the National Academy of Sciences*, 97(1), pp.103-108.
- Teh, W. T., Stern, C., Chander, S., & Hickey, M. (2014). The impact of uterine radiation on subsequent fertility and pregnancy outcomes. *BioMed research international*, 2014.

- United Nations Scientific Committee, 2000. UNSCEAR, sources and effects of ionization radiation, on the Effects of Atomic Radiation. Report to the General Assembly with scientific annexes, 1.
- Valerie, K. and Povirk, L.F., 2003. Regulation and mechanisms of mammalian double-strand break repair. *Oncogene*, 22(37), pp.5792-5812.
- Weintraub, N.L., Jones, W.K. and Manka, D., 2010. Understanding radiation-induced vascular disease. *Journal of the American College of Cardiology*, 55(12).
- You, Z., Chahwan, C., Bailis, J., Hunter, T. and Russell, P., 2005. ATM activation and its recruitment to damaged DNA require binding to the C terminus of Nbs1. *Molecular and cellular biology*, 25(13), pp.5363-5379.
- Youle, R.J. and Strasser, A., 2008. The BCL-2 protein family: opposing activities that mediate cell death. *Nature reviews Molecular cell biology*, 9(1), pp.47-59.
- Wang, Q., Stringer, J.M., Liu, J. and Hutt, K.J., 2019. evaluation of mitochondria in oocytes following γ -irradiation. *Scientific reports*, 9(1), pp.1-9.
- Wallace, W.H.B., Shalet, S.M., Hendry, J.H., Morris-Jones, P.H. and Gattamaneni, H.R., 1989. Ovarian failure following abdominal irradiation in childhood: the radiosensitivity of the human oocyte. *The British journal of radiology*, 62(743), pp.995-998.
- Wallace, W.H.B., Thomson, A.B. and Kelsey, T.W., 2003. The radiosensitivity of the human oocyte. *Human reproduction*, 18(1), pp.117-121.
- Ward, J.F., 1994. The complexity of DNA damage: relevance to biological consequences. *International journal of radiation biology*, 66(5), pp.427-432.
- Weber, K.J. and Flentje, M., 1993. Lethality of heavy ion-induced DNA double-strand breaks in mammalian cells. *International journal of radiation biology*, 64(2), pp.169-178.

Winship, A.L., Stringer, J.M., Liew, S.H. and Hutt, K.J., 2018. The importance of DNA repair for maintaining oocyte quality in response to anti-cancer treatments, environmental toxins and maternal ageing. *Human reproduction update*, 24(2), pp.119-134.

National Council on Radiation Protection and Measurements. Radiation protection guidance for activities in low-Earth orbit. Bethesda, MD: NCRP; 2000. Report No. 132